An experimental analysis regarding neural bases of hand synergies during reach-to-grasp movements

Alexander Warsi
Jessica Ericsson

Master Thesis in Biomedical Engineering
Department of Biomedical Engineering, Faculty of Engineering, LTH
Lund University

Advisors: Henrik Jörntell, Martin Stridh

February 12, 2018

Printed in Sweden
E-huset, Lund, 2018

Abstract

Traumatic brain injury and diseases causing cortical damage is a global problem. Despite their vast extent, their pathophysiology is poorly understood. It is however known that the loss of motor functions can be regained thanks to adaptive properties of the neuronal system. Early task specific motor training is proven to be critical for rehabilitation. We set out to better understand how the CNS controls hand movement to in the future be able to access optimal diagnosis and motor training succeeding cortical damage. The approach, being to reach experimental support to the theory that muscle synergies during reach-to-grasp type movements are mirrored by synergies in cortical activity, was put into effect with the use of a tracking device for hand movement called Leap Motion, and an EEG system. Simultaneous recordings from these two systems were made on subjects to document angles of the hand as well as EEG signals in the cortex during approximately 100 repeats of four different types of carefully designed reach-to-grasp movements. Correlations between specific angles of the hand during the movements were calculated and plotted, as well as correlations between all electrodes. PCA was performed on both data sets to evaluate the possibility of dimensionality reduction. The results revealed groups with similar correlation patterns in both angular and EEG data, as well as primary principal components with high eigenvalues for both data sets, supporting the documented notion of muscular synergies as well as the theory of synergistic behaviour in the CNS.

Acknowledgments

We would like to thank Henrik Jörntell (head of the neuroscience department, BMC, Lund) for giving us appreciated guidance throughout the thesis work, and Martin Stridh (associate professor, Ph.D. in biomedical signal processing, LTH, Lund) for supervising our work. We also want to thank Anders Wahlbom (Ph.D. student at the neuroscience department, BMC, Lund) for helping us with EEG setups, collection of EEG data and for serving as a test subject, as well as LTH students Erik Andersson and August Sundström for serving as test subjects.

Table of Contents

List of Figures

List of Tables

Abbreviations

CNS Central Nervous system

CT Computed Tomography

DIP Distal interphalangeal joints

DTI Diffusion Tensor Imaging

ECG Electrocardiography

EEG Electroencephalography

EGG Electrogastrography

EMG Electromyography

EOG Electrooptigraphy

MAC Motion Analysis Corporation

MEG Magnetoencephalography

MP Metacarpo-Phalangeal joints

MRI Magnetic Resonance Imaging

PC Principal Component

PCA Principal Component Analysis

PIP Proximal interphalangeal joints

Chapter 1

Introduction

This chapter explains the reason why this project was initiated. We introduce a background explaining why this work is important as well as highlighting its goals and purposes, giving the reader a general overview of the subject.

1.1 Background

Traumatic brain injury is reported at all ages. It is a leading cause of death and long term disability among people younger than 45 years of age. In 1990, there was an estimated 9,500,000 cases of traumatic brain injury worldwide requiring medical care or resulting in death. Despite its vast frequency, pathophysiological mechanisms of traumatic brain injury remain poorly understood. [1]

Stroke is also a common neurological threat in the western world. According to the World Health Organisation, 15 million people per year worldwide suffer a stroke. After coronary heart disease and cancer, it is the third leading cause of death. A stroke, causing interruption of blood supply to the brain or intracranial bleeding, often leads to dysfunctionality of the affected vascular territories, and ultimately necrosis. Therefore, if not resulting in death, a stroke often causes disability in a variety of forms. [2]

When suffering a head trauma, stroke or certain degenerative brain diseases such as dementia, Alzheimer's disease and many more, damage is often located to the cortex of the brain. Large areas of the cerebral cortex represent the coordination of motion and sensation in the hand. In the motor cortex, the area devoted to the hands approximately equals the total area devoted to arms, torso and legs. [3] In most cases of occurred cortical damage, motile abilities of patients are affected. However, the brain has an intrinsic capacity to compensate for structural damage by reorganising surviving networks. These processes are fundamental for recovery

of function after the mentioned forms of brain injury. Functional neuroimaging techniques have allowed the investigation of these processes in vivo. Loss of motile function after brain damage can thus be regained by proper treatment. [2]

A critical factor for cortical reorganisation and recovery seems to be task-specific practice of mobility. In healthy animals, it can be seen that immobilisation of a limb for several months leads to reorganisation of the neuronal network in the cortex representing the limb. More importantly, the reorganisation phenomena are reversible after cancelling the immobilisation and commencing motor training. These results demonstrate the adaptational abilities of the cortex when restricting movement, as well as the impact of motor training. [4]

In another study, it was shown that after ischemic damage to the cortical hand motor area, monkeys receiving four weeks training of hand use expanded cortical representations of fingers, wrist and forearm into intact cortex that had been formerly occupied by the elbow and shoulder representation. On the other hand, monkeys that did not receive training of hand use experienced a loss of the finger and wrist-forearm representation area in the surviving cortex. These findings emphasise the importance of early rehabilitative training for desired functional recovery following brain damage. [5]

Regarding cortical brain damage as in humans, diagnosis and rehabilitation is heavily dependent on the knowledge and experience of the physician in practice. The reason is that the methods used for diagnosis today are medical examinations by physicians and body scans that show only anatomy and not sufficient neurological function. Morgenstern *et al.* conducted a population based study where the results argue for a system with neurology support so that proper decisions regarding stroke therapy can be made [6]. Today, we lack a quantitative measure of brain function suited for this purpose. Tools for imaging such as CT, MRI and DTI are used, but the sampling rate and obtained information is not sufficient for optimal analysis of damage. It has been shown that early task-specific practice of mobility is a critical factor for cortical reorganisation and recovery after cortical damage [4, 5]. A more systematic, general and accurate method of diagnosing brain damage is needed to access optimal recovery of brain function after damage in the brain cortex [1].

1.2 General purpose of the project

The purpose of this project is to contribute to research intended to lead to an increased understanding of how the CNS controls hand movements. In the long term, this can potentially be used to develop improved methods of diagnosing and rehabilitating patients with cortical brain damage.

1.2.1 Specific goals

The specific goal of this project is to examine whether muscle synergies used during reach-to-grasp type movements are mirrored by synergies in the brain activity. By exploring this possibility, the thesis aims to contribute to future studies regarding how the CNS controls hand movement. This main objective was split into partial goals providing a more straightforward way to track progress as well as giving a structured overview for all parties involved. The goals are presented in the form of sections in upcoming chapters:
- Initial analysis of test data
- Design of reach-to-grasp movements
- Simultaneous collection of Leap Motion and EEG data
- Separate data analysis
- Matching Leap Motion and EEG data

Chapter 2

Theory

2.1 Anatomy and physiology of the CNS

The CNS is the part of the nervous system consisting of the brain and the spinal chord. Essentially, the cellular composition of the CNS is nerve cells and glia cells (astrocytes, oligodendrocytes, ependymal cells and microglia). The nerve cells have a cell body where the nucleus is located. Dendrites and axons emerge from the cell body to form a network. The nerve cells are responsible for the transmission of information in the nervous system and to enable this, contact between the nerve cells is essential. Contact is achieved through synapses formed between an axon terminal of one neuron and a dendrite or cell body of another neuron. See figure 2.1. The synapse is a structure that permits a neuron to send an electrical or chemical signal to another neuron. [7, 8]

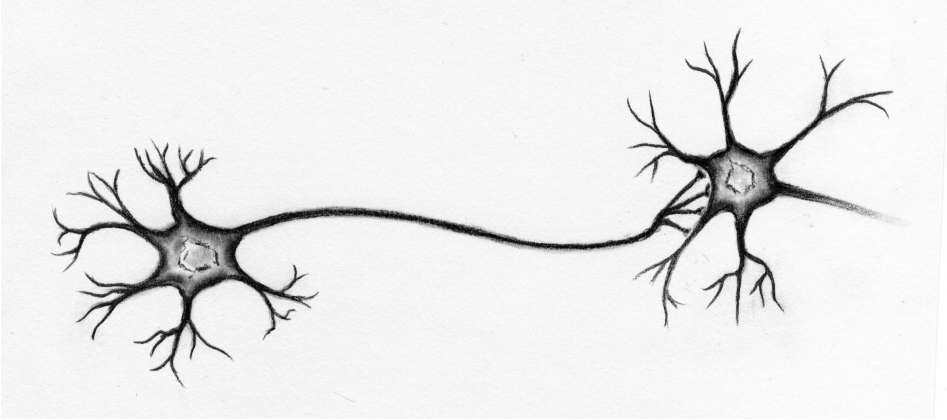

Figure 2.1: Two neurons and the connections formed between them through synapses.

If the membrane of a neuron is penetrated with a micro electrode, a resting potential of 60-70 mV can be recorded intracellularly. Synaptic activity causes fluctuations in this potential. Certain excitatory fluctuations give rise to action potentials that travel along the axons and allow nerve cells to communicate with each other. [8] The communication of the nerve cells leaves a trail of electrical activity that can be measured on the scalp with an EEG system. This will be further described in section 3.2.

2.2 The human hand

As can be seen in figure 2.2, the bones in the hand are plentiful. For this particular study, we focus on the fingers. The fingers are comprised of four bones each with the thumb as an exception, which contains only three bones. The bones closest to the wrist are called metacarpals. The metacarpals are followed by the phalanges. There are three phalanges in each finger except the thumb: proximal (closest to the metacarpals), intermediate (middle) and distal (furthest from the metacarpals). The thumb lacks the intermediate phalange. [10]

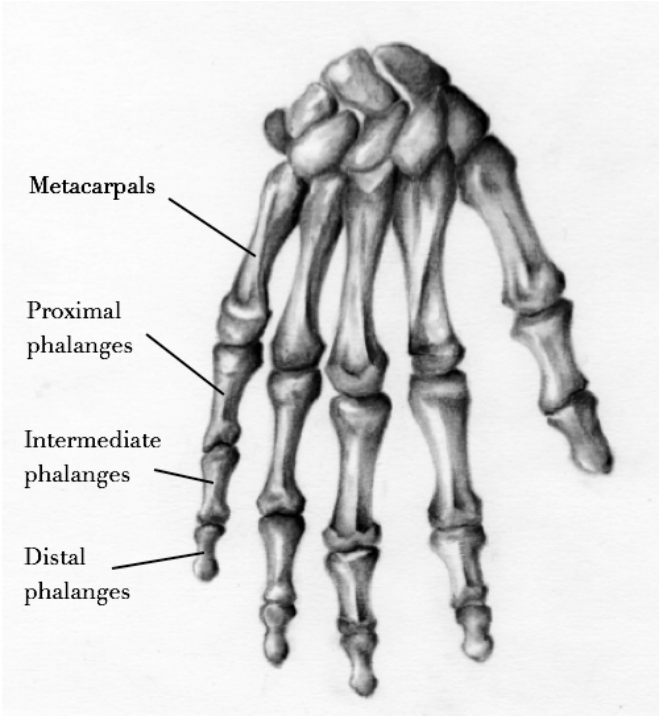

Figure 2.2: Bones of the fingers in the human hand.

The connections between the bones in the fingers form joints. The joints between the metacarpals and proximal phalanges are called metacarpo-phalangeal (MP). The proximal and intermediate phalanges form the proximal-interphalangeal joints (PIP) and the intermediate and distal phalanges form the distal-interphalangeal joints (DIP). See figure 2.3. [3]

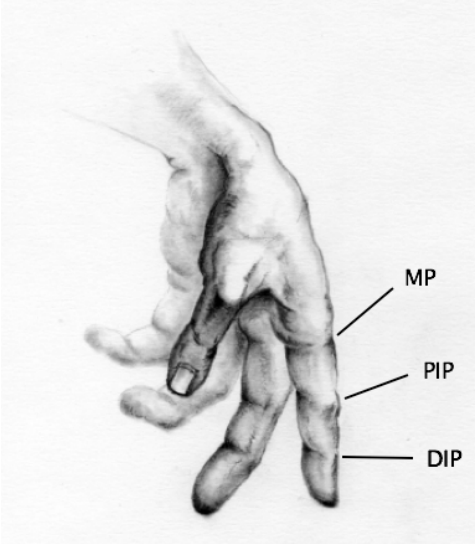

Figure 2.3: Joints in the fingers of the human hand.

2.3 Hand movement and grasping

The structure of the human hand, with its intricacy of bones, muscles, tendons, blood vessels and nerves, is a product of a long evolution. At functional level, the hand has evolved into a dynamic structure that combines rich sensory components and strength: it handles the scalpel of a neurosurgeon as well as the hammer of a blacksmith.

Provided the highly sophisticated structure of the hand, a seemingly infinite variety of movement patterns can be achieved. The disproportionately large area in the cortex devoted to the hands ensures great potential of learning new activities and coordinated hand movements. [3]

As infants, we mostly use our hands as sensory organs to explore environmental properties around us. As we grow and the CNS continues to mature, we start using our hands as motor organs to grasp objects and pre-shape our hands before doing so depending on the dimensions of the object. We perform reaching movements frequently and effortlessly, for example when eating food or using a tool. Because

of the critical role that the hands play in daily activities, many studies have been conducted to characterise the way the CNS controls the motions of the hand. The seemingly simple task of grasping an object contains a highly complicated cooperation of our muscles, bones and joints that is initiated in the CNS. [9] Studies conducted so far provide a comprehensive, although incomplete, picture of the neural mechanisms underlying object grasping. As one could expect, the CNS behaves differently when grasping an object depending on the physical properties of the object (*i.e.* its size and shape), affecting the pre-shaping of the hand. However, the subject could grasp the same object with different end goals, for instance in order to eat it or to place it in a basket. Thus, the same grip can be used to attain different action goals. It is noteworthy that recent studies show that grasping neurons in monkeys can be differentially activated depending on the action (grasp-to-eat or grasp-to-place) in which the coded act is embedded. [11]

The opposing thumb is especially important for grasping purposes. The versatility of the thumbs lies in its flexion-extension patterns and the adjustable rotatory plane in which the flexion-extension can take place. This allows the thumb to act in any plane necessary to oppose the other fingers. [12]

Given the large variety of possible prehension patterns, it is sufficient to describe the principal types of patterns for analytical purposes. Figure 2.4 shows an example of grasping classification in the form of six basic types of grips, defined by G. Scheslinger in 1919. [12]

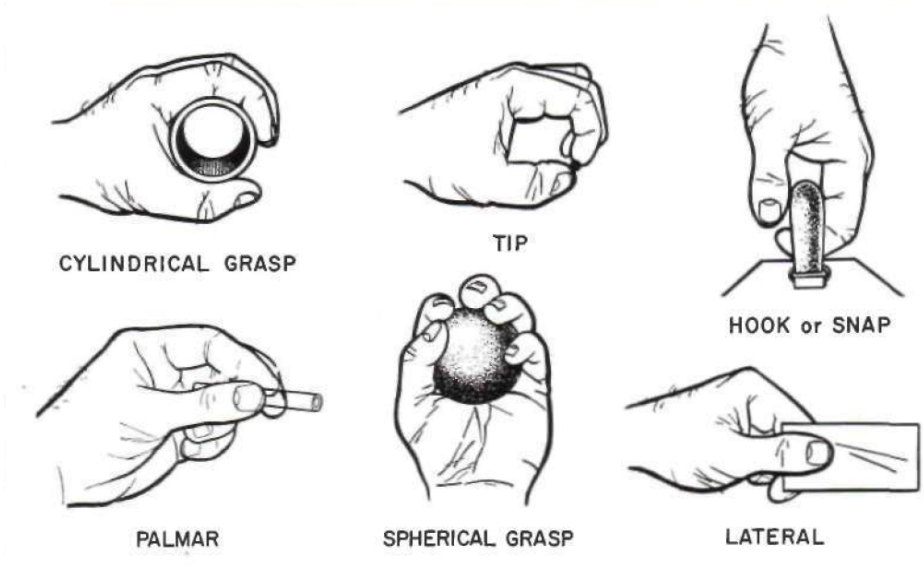

Figure 2.4: Six basic types of grips defined by G. Scheslinger in 1919. [12]

2.4 Synergies

The human hand has so many degrees of freedom that it may seem impossible to control. A potential solution to this problem is ”synergy control” which combines dimensionality reduction with great flexibility. Synergy is a concept where multiple elements work together towards a common goal. It has been extensively used in studies to understand neural control of movement, and for applications of neuro-rehabilitation. In recent years, robotics have applied the framework of synergies to design and control concepts for robotic hands and prostheses. [9]

Synergies have been shown to be active on several levels, including (but not limited to) neural, muscular, joint and on movement trajectory level. At the level of neurons, neural input could be viewed as a form of synergistic control as it constraints the timing at which multiple motor units are activated. [13] Kinematic and kinetic analysis of reaching have shown invariant features suggesting that the CNS relies on simple rules for movement planning and execution.

On muscular and joint level, muscle synergies have been defined as patterns of muscle activity whose timing and/or amplitude modulation enable the generation of different movements. The dynamic relationships between muscle activation and joint torques, and between joint torques and joint motions are complex and non-linear. [14] The synergy term has been used in several contexts when describing thumb and finger movements, often referring to observations of movement patterns that are characterised by simultaneous motion of the fingers in the early stages of a grasping motion, and for the purpose of classifying hand movements or grasp postures. Studies of isolated finger movement (for instance when typing) and movement sequences involving motion of one or more digits (piano playing or finger spelling) have found that during isolated finger movement, motion that is not necessary to complete the task also occurs at other fingers in a subject-dependent but stereotypical fashion. This type of movement is called corollary movement. The degree of movement correlation across pairs of digits is stronger for adjacent than non-adjacent digits. The studies have also reported that corollary movement is not obligatory considering biomechanical constraints of the hand. These observations have lead to the suggestion that synergistic finger motions would simplify the problem of controlling the large number of degrees of freedom inherent in motion of all of the fingers of the hand. [15]

Figure 2.5 shows an illustration of how muscle synergies are known to work. It shows a pattern of co-activation of muscles recruited by single neural command signals. As illustrated, one muscle can be part of multiple muscle synergies, and one synergy can activate multiple muscles. [15]

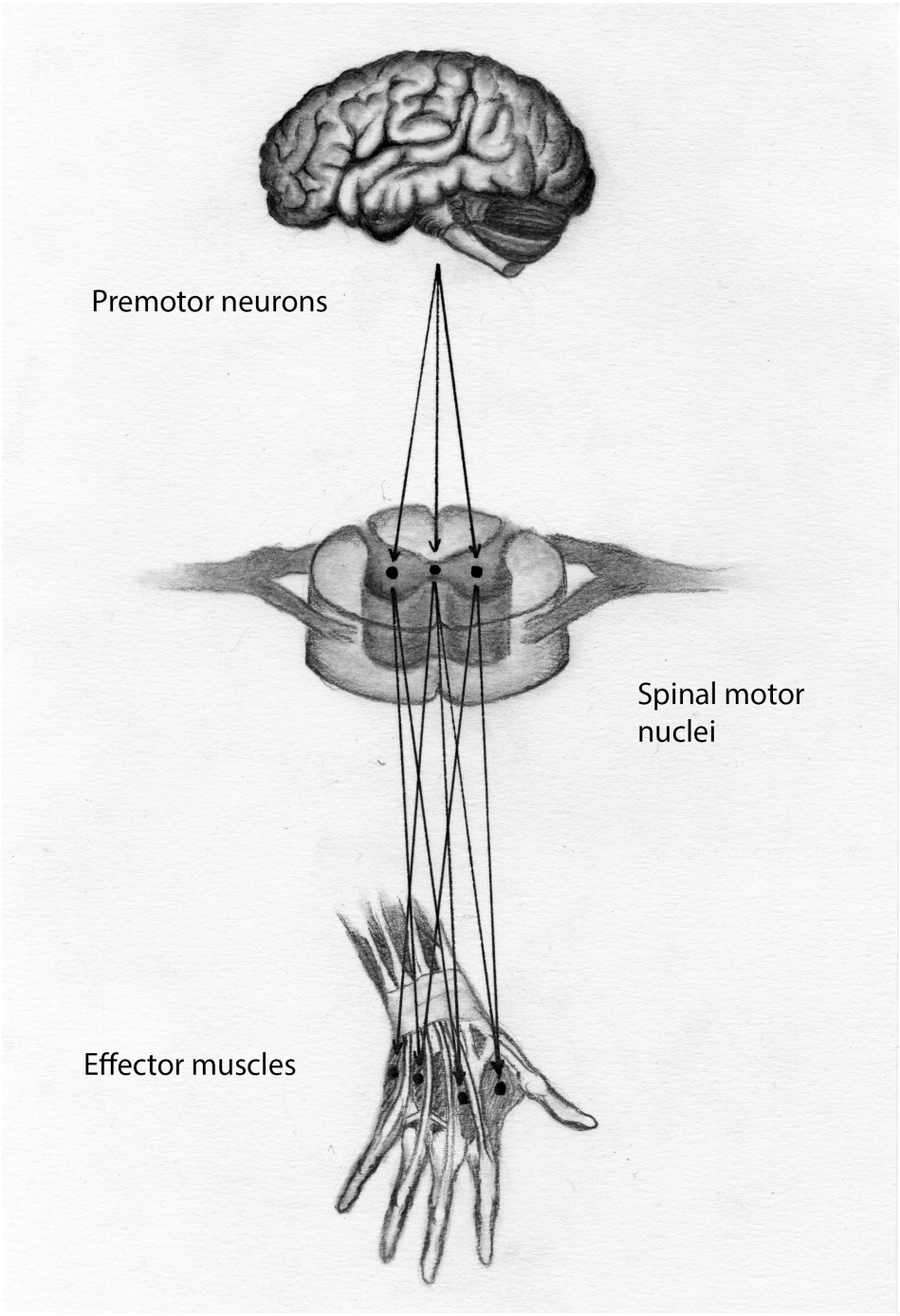

Figure 2.5: An illustration of muscle synergies controlled by single neural command signals.

Regardless of the level on which the synergy exists, the main implication shared across the levels is that multiple degrees of freedom are controlled within a lower dimensional space than the available number of dimensions. The combination of synergies as a whole allows normal movement. Injury to the nervous system would interfere with the ability of the system to flexibly combine synergies, thus leading to abnormal synergies. [9]

Existing research suggests that muscle synergies are building blocks used by the CNS to control goal directed movement. However, regularities may derive from optimisation of the task. Although theories exist, as for now there is no direct documented evidence for muscle synergies as centrally organised building blocks in the CNS. This support would come from identifying the neural substrates of the muscle synergies, which would help to clarify whether muscle synergies are merely low-dimensional approximations of the muscle patterns or building blocks organised by the CNS. [14] This uncertainty is mainly what we attempt to shed a light on in this thesis.

2.5 Motor control

As mentioned in section 2.4, synergies related to motor control exists on several levels. A central problem in the neural control of multi-joint movement is the degree of freedom problem: given the seemingly infinite number of mechanical degrees of freedom of the human movement system, how does the nervous system organise and simplify the control of these degrees? In 1967, N. Bernstein concluded that at higher levels of the nervous system, spatial aspects of movements are controlled rather than the action of specific joints of muscles, meaning that the neural command for hand movements is formulated in terms of trajectories of the hand in space. [16] The underlying notion in this and many other studies of motor control is that the more invariant and simple an ensemble of movement trajectories is, the more likely it is that the nervous system employs that reference frame. In other words, control in this conception refers to stabilisation of a movement. By implication, lack of control means reduced stability and less regularity of the movement. [17] Kinematic regularities observed at the level of the end-effector are interpreted as evidence for end-effector control, and kinematic regularities at the level of the joint configuration are interpreted as evidence for joint-level control. A similar argument can be made for yet other levels, such as patterns of EEG or of joint torques. [18]

2.6 Principal component analysis

PCA has its origin in work by Karl Pearson around the turn of the 20th century [19], and was further developed and named in the 1930s by Harold Hotelling. [20] It is a technique for reducing the dimensionality of large datasets, thus increasing its interpretability and preserving the information of the data. It needs no distributional assumptions, although multivariate normal (Gaussian) distribution of data sets is usually assumed. Since the statistical information of data lies in its variability, PCA finds new uncorrelated variables (principal components) from correlated ones through maximising the variance of the data. These PCs are linear functions of the original variables and they depend on the data set at hand rather than being pre-defined, meaning that they are signal dependent. [21]

Each PC contains new information about the data set. They are ordered so that the first few components account for most of the variability in the data. In signal processing applications such as ours, PCA is used on time samples rather than on a data set of variables. Another way of describing PCA is that it's an orthogonal rotation of the space in which the data set is presented. The first axis of the transformed coordinate system accounts for the maximal variance of the data set, the second axis to the maximal variance in the direction orthogonal to the first axis, and so on. The emphasis on variance stems from the observation that high variance corresponds to interesting dynamics of a signal, while low variance usually corresponds to noise in the system. [22]

PCA can be based on either the covariance matrix or the correlation matrix of the data set. The correlation matrix is obtained by multiplying the data set matrix with its transpose. Finding the PCs translates into solving an eigenvalue/eigenvector problem of the correlation matrix. The eigenvector corresponding to the largest eigenvalue constitutes the first PC, the second order eigenvector constitutes the second PC and so on. Once obtained, the PCs can be further used for facilitated analysis of the data set. [21, 22]

Chapter 3

System

This chapter provides an overview of the hardware and software used during the progression of the project.

3.1 Leap Motion

The Leap Motion Controller (see figure 3.1) is a motion capture device that tracks hand, wrist, forearm and elbow positions. Benefits such as low cost, user friendliness, portable size and open source documentation/coding has lead to a rapidly occurring integration of the device into health-care applications and research. The open source documentation allows potential of specifying use of the controller. [23]

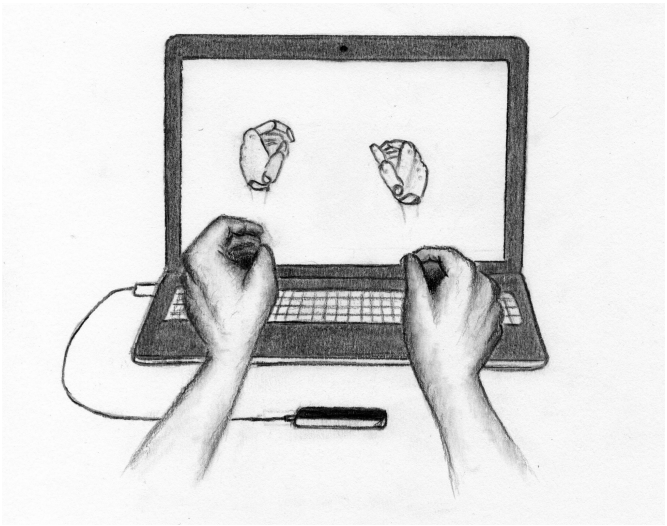

Figure 3.1: The Leap Motion Controller, a marker-less motion sensing system designed to quantify hand movements and gestures.

The controller consists of two cameras and three infrared LEDs. These components track infrared light with a wavelength of 850 nm. [25] A hand observed by the system is tracked within a three dimensional space above the controller. The system employs a right-handed Cartesian coordinate system. See figure 3.2 for an illustration of the axes of the coordinate system relative to the controller. [24] The sensors are directed along the y-axis, i.e. upwards from the sensor and they have a field of view of about 150 degrees. The effective range of the Leap Motion Controller extends to up to 60 centimetres above the device. [24]

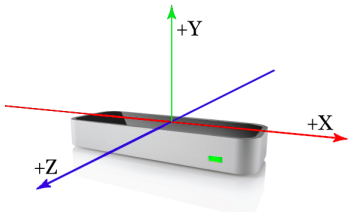

Figure 3.2: The Leap Motion Controller with and illustration of its tracking coordinate system. [24]

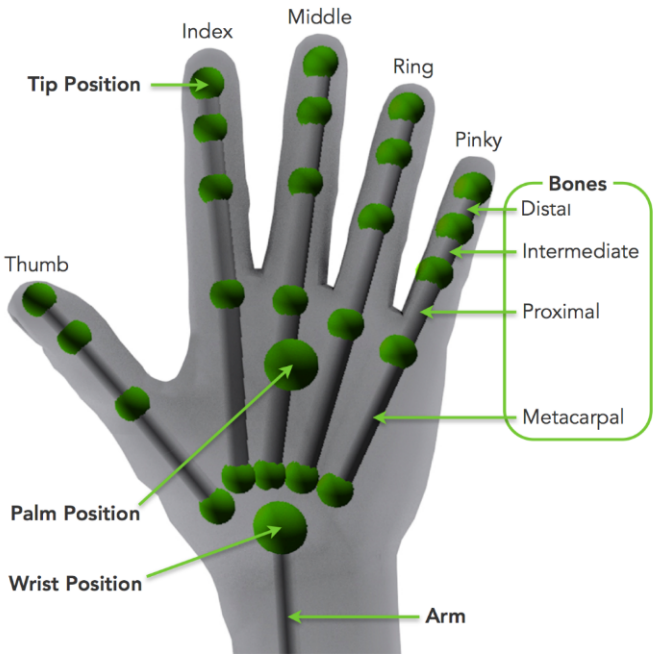

Figure 3.3: Available positional tracking data through the Leap Motion application programming interface. [26]

See figure 3.3 the positional tracking data of the hand available through the application programming interface. Every tracked entity in the Leap Motion interaction space falls within a hierarchy that starts with the hand. The system allows tracking of all bones shown in the figure, along with positional information of all joints in the hand, palm, wrist, forearm and elbow. [26]

A. Smeragliuolo *et al.* conducted a study in 2016 validating its ability to quantify three types of hand movements as well as three types of hand positions, see figure 3.4. They compared the tracking data with a marker-based motion capture system from MAC by studying correlation. Wrist flexion/extension and radial/ulnar deviation showed good overall correlation (95% and 92% respectively) with the MAC system. However, when tracking forearm pronation/supination, there were inconsistencies in reported joint angles with a correlation of 79%. Additionally, performing movements with a loose or tight fist resulted in data with significantly lower quality than open hand movements. [23] This has to be taken into account when designing hand movements for research.

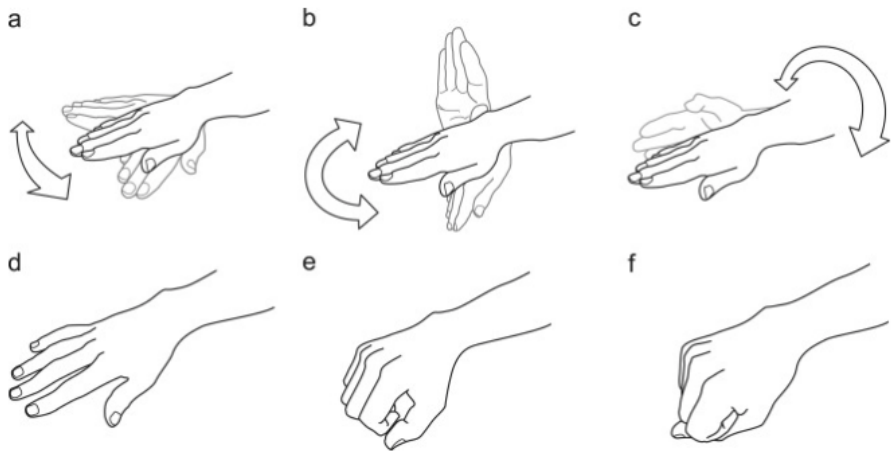

Figure 3.4: Hand movements: a) radial/ulnar deviation, b) flexion/extension, and c) supination/pronation. Hand positions: d) open hand, e) loose fist, and f) tight fist. [23]

3.2 EEG equipment

Modern medicine allows a number of electrophysiological techniques to analyse the functions of the human body. One group is electrobiological measurements such as EEG (brain) along with ECG (heart), EMG (muscular contractions), MEG (brain, magnetic), EGG (stomach) and EOG (eye dipole field).

The EEG is a technique that allows measurement of scalp electrical activity generated by brain structures. The electroencephalogram is defined as electrical activity of an alternating type recorded from the scalp surface after being picked up by metal electrodes through conductive media [27]. Since it is measured on the surface of the head, it is a non-invasive procedure that can be repeatedly applied to all kinds of patients with minimal risk and limitation. [28]

The EEG measures mostly the currents produced during synaptic activity (described in section 2.1). Only large populations of neurons can generate activity strong enough to record on the skull. In order to reach the electrodes on the surface, the currents need to penetrate the skin, skull and several other layers. The electrical signal is weakened during the transport and therefore needs to be massively amplified before being displayed on paper or stored to computer memory. [29] Since EEG reflects both normal and abnormal electrical activity of the brain, it is a powerful tool in the field of neurology and clinical neurophysiology. [28]

Electrical activity of neurons forms wave shapes that commonly are sinusoidal. They normally range from 0.5 to 100 μV in amplitude peak to peak. The brain state of the individual may make certain frequencies more dominant at times. Brain waves are categorised into four basic groups, see figure 3.5: beta (>13 Hz), alpha (8-13 Hz), theta (4-8 Hz) and delta (0.5-4 Hz). The most extensively studied frequency of the human brain is the alpha rhythm. Alpha activity is induced by relaxation and closing of the eyes, and abolished by eye opening or alertness by mechanisms such as concentrated thinking. During normal awake state beta waves are dominant and when sleeping the power of lower frequency bands increase. [28]

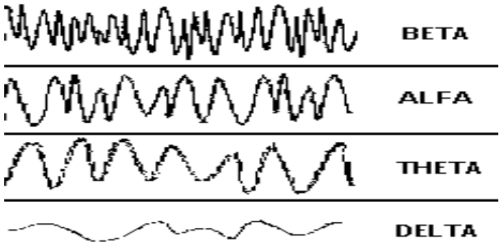

Figure 3.5: Brain wave samples with dominant frequencies belonging to beta, alpha, theta, and delta band. [28]

Several types of events such as a hand movement result in the generation of event-related potentials, synchronisations and desynchronisations which can be seen in measurements of electrical activity . Averaging techniques are often used in order to detect event-related potentials since the procedure enhances the signal-to-noise ratio. [30] See figure 3.6 for an average of recordings from 60 finger movements and 60 foot movements made by C. Toro *et al.* The data is an average of 60 self-paced movements for both finger and foot movements. Frequency of movement was approximately 0.1 Hertz. [31]

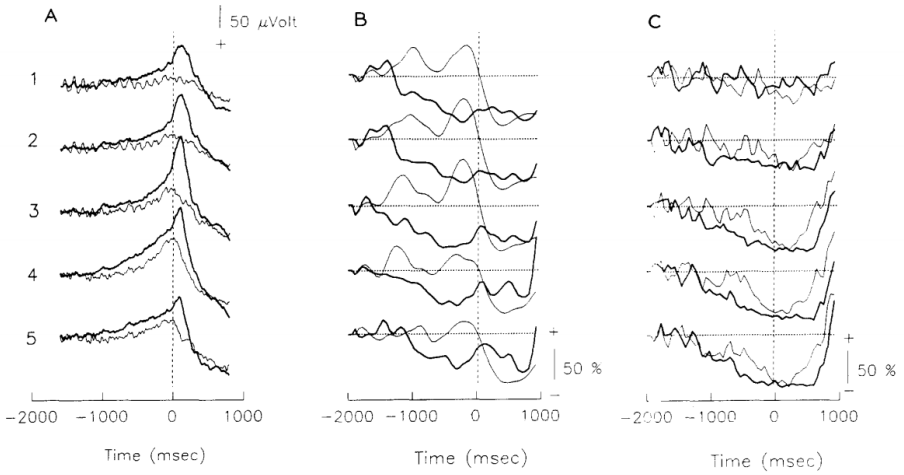

Figure 3.6: (A) Movement-related cortical potentials, (B) 10-12 Hz event-related desynchronisation and (C) 20-30 Hz event-related desynchronisation responses recorded from 5 electrodes to finger movements (thick lines) and foot movements (thin lines) in a patient. [31]

H. Agashe *et al.* conducted a study in 2015 where EEG and hand kinematics were simultaneously recorded during tasks of object grasping. The purpose was to quantify the EEG information by measuring its ability to discriminate between the grasp types. Kinematics were segmented consistent with the EEG and PCA was used to decompose the joint angular velocities into kinematic synergies across all trials. In this study, they found high decoding accuracy's far above chance levels for both joint angle velocities and their synergies, see figure 3.7. These findings are significant not only as evidence for time-domain modulation in macro-scale brain activity, but for the field of brain-machine interfaces as well. They may provide a means of extracting information about motor intent for grasping without the need for penetrating electrodes, and also suggest that it may soon be possible to develop non-invasive neural interfaces for the control of prosthetic limbs. [32]

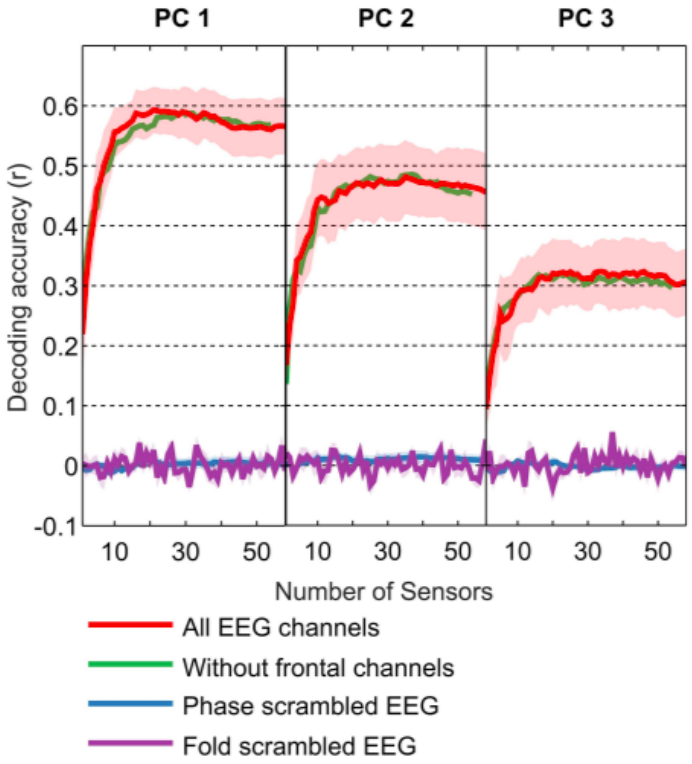

Figure 3.7: EEG decoding accuracies for the first three PCs of hand movement found in the study of H. Agashe *et al*. Mean decoding accuracies across subjects are shown in red for PC1, PC2 and PC3. [32]

Chapter 4

Method

This chapter, as well as the following chapter with results, are structured chronologically by following the five main goals of the project (mentioned in section 1.2.1). A recap of the goals with brief summaries of methods follows:

- Initial analysis of test data
  - Focusing on Leap Motion, previously recorded hand coordinates during repeats of movements were extensively studied in MatLab with the aim of finding flaws and optimising both data collection and data analysis of hand movements. New small scale Leap Motion recordings were conducted to solve discovered problems, test new theories and apply calculations.
- Design of reach-to-grasp movements
  - Appropriate reach-to-grasp movements were designed for subject trials. A high variation of movement types was aimed for with respect to limitations of the Leap Motion controller.
- Simultaneous collection of Leap Motion and EEG data
  - The designed reach-to-grasp movements were performed by subjects while recording and saving both Leap Motion and EEG data.
- Separate data analysis
  - Leap Motion data: useful parameters were imported from the Leap Motion data recorded during subject trials, parameter data from movement repeats were cut out from the continuous data, angles of the hand were calculated and extracted from this data, angular correlation coefficients were calculated and plotted at fixed samples and over time, PCA was performed.

  - EEG data: the EEG data outside the time-span of the Leap Motion recording was cut out and discarded, the EEG data during the movement repeats were segmented out and saved for use, the signal was filtered to reduce noise, correlations between electrodes were calculated during the movement repeats, noisy electrode data was removed, electrode correlations were plotted at fixed samples and over time, PCA was performed.

- Matching Leap Motion and EEG data
  - Temporal correlation coefficient plots from Leap Motion and EEG data were visually compared to analyse how to match the two data sets and proceed with future synergy studies.

The complete method description of each goal is presented in its own section ahead.

4.1 Initial analysis of test data

Computations, data processing and plotting were performed using MATLAB (The MathWorks Inc., USA). Data sets from the Leap Motion controller as well as the EEG system were saved in formats compatible with this program.

4.1.1 Analysis of pre-existing data

Visualisation of Leap Motion data previously collected(by the department of neural bases of sensory motor control at BMC, Lund) for three different reach-to-grasp type movements (a precision grip of a small desk lamp, power grip of a pen and grasping of a round lid with all finger tips) revealed several problems regarding upcoming analysis. Primarily the coordinate system seemed to fluctuate, creating a deviation in the end point coordinate location of a hand movement even though it spatially never changed. With deviating end point coordinates the repeats of a movement would not be relatable to each other since the end goal of a reach-to-grasp movement is the only consistent spatial feature within each type of the movement. This feature of the system would greatly interfere with future analysis since the tracking data would need to be manipulated (without distorting the information) to reach a conformed end point. Attempts were made to find a general and automatic way to decide the end points of each repeat from the raw data. This task was particularly difficult since there is no guarantee that the hand will behave in a certain way during a movement, or stay within any pre-set boundaries. This lead to the decision to manually identify and select the

termination points by visualising the Leap Motion data in a predictable spot on the hand. For instance, when performing precision gripping, the tip of the index finger would seemingly be good spot to look at since its coordinates in space should show an abrupt stop when reaching the final destination. Despite using plots of predictable joint coordinates, it proved difficult to determine the exact location of the end point in the data. For this reason, a small sample window around these selected points were used to align the trajectory of each repetition of the movement with the initial one. The alignment was made with Procrustes analysis using a simple linear transformation consisting only of orthogonal rotation and translation. In this case, the transformation *T(X)* was from $R^3 \rightarrow R^3$ and can be described by equation 4.1, where t is the translation vector and R is the rotation matrix.

$$T(X) = t + RX \tag{4.1}$$

This way, the transforms of each repeat of the movement were found to optimally match the end point of the initial iteration in space. These transforms were then applied to the entire movement trajectories which were successfully moved and matched in space, resulting in conjoined end points. However, visualisation revealed an unwanted amount of deviation in the rest of the movement. In addition, the displacement of the trajectories seemed to distort the information. For this reason, a simpler approach was chosen. The fluctuation of the coordinate system seemed to be the result of the hand leaving the field of vision of the Leap Motion device between each event. Consequently, in order to avoid the problem during future data collection, the movements were to be designed so that the hand stays within the field of view for the entire duration of a recording session.

Another problem discovered during this phase of testing was the amount of noise and glitches in the Leap Motion data. This issue was partly dealt with through the solution to the previous problem. However, glitching often occurred at the termination point of the movements since some tracking points (such as the finger tips) would be blocked by the grasped object. Certain hand positions also revealed glitching due to the limitations of the controller mentioned in section 3.1 and 4.2, mainly during pronation and supination of the hand or when making a fist. This problem was avoided by designing hand movements with minimal intent of pronation/supination. The glitches at the termination points proved more difficult to deal with since it was impossible for all tracking points to be visible during the grasping moment. However, the target of analysis is the pre-shaping of the hand before grasping. Consequently, information at the absolute end of a movement and the moment of actual grasping could be discarded, making glitching during this phase irrelevant. Therefore, movements that include creating a fist at the

grasping moment could be used despite this. This conclusion was helpful since it allowed a broader spectrum of grasping types for data collection and analysis.

4.1.2 Small scale data collection

To further prepare for the simultaneous data collection described in section 4.3, different movements were tested while being tracked with the Leap Motion controller and evaluated during this phase. As previously mentioned, the end-points had proven to be difficult to pin point because of different tracking points being blocked by the grabbed item. As the whole hand was visible and no tracking points blocked at the starting phase of each repetition, these points were much more distinct. Consequently, it was decided that the starting phases of each movement repetition would be used to mark and extract movement trajectories.

Initially, a lot of testing was performed with the coordinates of a hand during movement. This seemed natural since the coordinates showed the trajectory of the hand. When visualising the coordinates in a 3D plot, it was discovered that there was a lot of deviation within each type of movement since the position of the hand in space is not reproducible. This problem was solved through the realisation that looking at the angles of the joints together with the angles between adjacent fingers, as well as the roll, pitch and yaw of the hand sufficiently describes the pre-shaping of the hand while eliminating the dependency of hand localisation in space. As seen in figure 3.3 in section 3.1, the Leap Motion controller tracks the positions of all joints in the hand in the form of coordinates in a 3D space. The spatial whereabouts of the bones that form the fingers is also obtainable in the form of vectors through programming. Since joint angle is not a feature directly available through the Leap Motion programming interface, they were obtained through calculations in MatLab. An open source java-code for tracking and printing the coordinates of all joints in the hand, position of the palm, wrist and elbow, roll, pitch and yaw was found. Using the open source documentation of Leap Motion as a basis, this code was modified to find the bone vectors and store them along with the pre-set features. The bone vectors were used to calculate targeted angles of the hand using linear algebra.

To proceed with the analysis, 50 repetitions each of three distinct reach and grasp type movements were evaluated by tracking the movements and creating scatter plot matrices from the recorded data. This was done to verify that the movements were distinguishable and that changes of different angles of the hand were correlated with each other.

4.2 Design of reach-to-grasp movements

Since the tracking of the Leap Motion controller is done with the help of cameras and LEDs directed upwards from the position of the controller, anything behind the initial target is impossible to track with absolute certainty. The controller uses algorithms and interpolation to estimate the positions of body parts outside its field of vision. This is a major limitation of the controller. As described in section 3.1, forearm pronation/supination and fist formation should be avoided to maximise tracking accuracy. This was important to consider when designing movements for further analysis. Variations in joint angles, roll/pitch/yaw and in angles between adjacent fingers were highly considered when designing the movements. Four different types of grasping movements were designed with requirements and tracking limitations taken into account.

4.3 Simultaneous collection of Leap Motion and EEG data

Four subjects participated in the simultaneous data collection of EEG and Leap Motion data. Setup of objects (pencil/bottle) used as targets of grasping were prepared as shown in figure 4.2. Subjects were instructed how to perform the four designed reach-to-grasp movements shown in section 5.2. EEG equipment was attached to the scalp of the subjects according to instructions from the EEG system manufacturer (128 electrode Geodesic Sensor Net), see figure 4.1. Electrode impedance was measured and electrodes showing poor conduction were moistened with a pipette to optimise conductivity. EEG system calibration was performed prior to each recording. When comparing collected data from EEG and Leap Motion, it is essential that they can be related to each other in the time domain and if they can not, there is no way to find useful correlations between EEG signals and hand movements. Therefore, time stamps were checked when testing Leap Motion data collection to make sure the time-line during each session was continuous and didn't reset due to any events. In order to temporally match the two data sets created during each trial, a timestamp mark was manually generated in the EEG files as soon as the Leap Motion data collection started, as well as at the moment it finished. Subjects performed approximately 100 iterations of each reach-to-grasp movement, resulting in four sessions per person. They were instructed to perform grasping as intuitively as possible with minimal thinking activity and concentration to minimise interfering signals from irrelevant cortical activity.

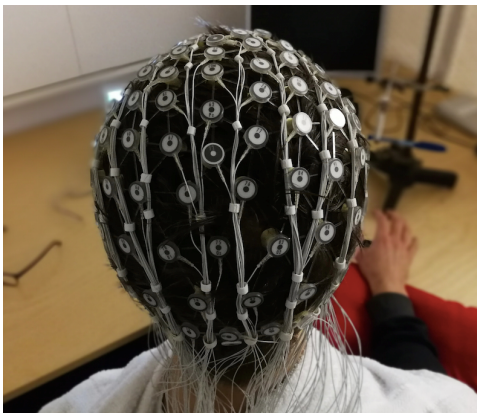

Figure 4.1: Subject with attached EEG electrodes.

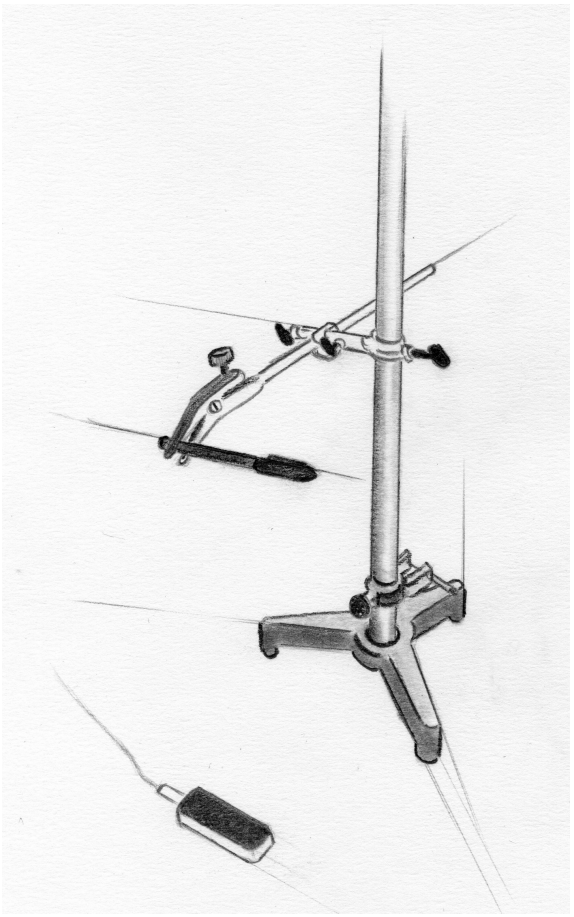

Figure 4.2: Illustration of the setup with a pen as grasping target.

4.4 Separate data analysis

Here follows a description of how the data files from the final collection of Leap Motion and EEG data were processed and analysed. Each flow chart is followed by a more detailed description of the involved steps.

4.4.1 Leap Motion

Figure 4.3 gives an overview of the processing performed on data from the Leap motion device during the simultaneous data collection described in section 4.3.

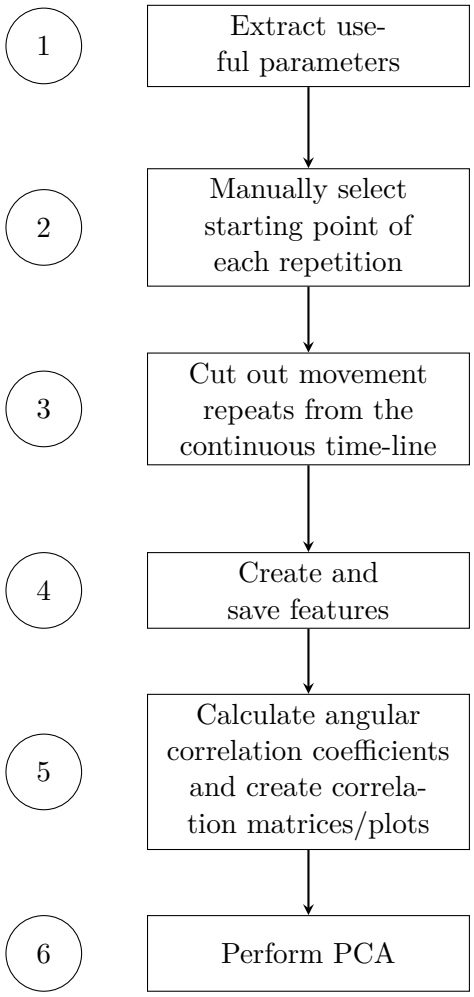

Figure 4.3: Flow chart of Leap Motion data processing.

Step 1 - Extract useful parameters

The raw data files from the Leap Motion recordings during the reach-to-grasp movements by the subjects contained a substantial amount of tracking information. They were loaded into MatLab in the form of large matrices with all available features represented column-wise and each sample represented by a row in the matrix. The pitch, roll and yaw of the hand, thumb fingertip positional coordinates as well as the bone vectors for the whole hand were imported from the matrices of each subject and saved for further analysis.

Step 2 - Manually select starting point of each repetition

The xyz-coordinates of the thumb finger tip of each subject were plotted. The initiations of each movement repetition were identified through these plots, and marks were manually created at the initiation points. In this way, vectors with temporal information of movement starting points were obtained to be used for isolating the information of each movement repeat (in step 3) from the continuous data.

Step 3 - Cut out movement repeats from the continuous time-line

It was assumed that each movement repeat took approximately the same amount of subject-dependent time to perform in each recording trial. Hence, the Leap Motion information from each starting point up to a fixed number of sample points ahead was extracted and saved. The number of samples for each movement type and each subject was determined by using the thumb finger tip coordinate plots with the marked initiation points mentioned in step 2 and additionally marking the perceived middle of the end point location area in order to calculate the average of all repeats. Data describing the period after the point of contact, including the retraction of the hand to the initial position, was thereby discarded, leaving only the pre-shaping trajectory information.

Step 4 - Create and save features

The bone vectors from the extracted movement information were used to calculate the joint angles as well as the angles between adjacent fingers. Since the tail of each obtained subsequent vector started at the head of the previous one (see figure 4.4), the joint angles were calculated using equation 4.2. The angles between adjacent fingers were calculated by simply using the dot product between the metacarpal bone vectors of each finger.

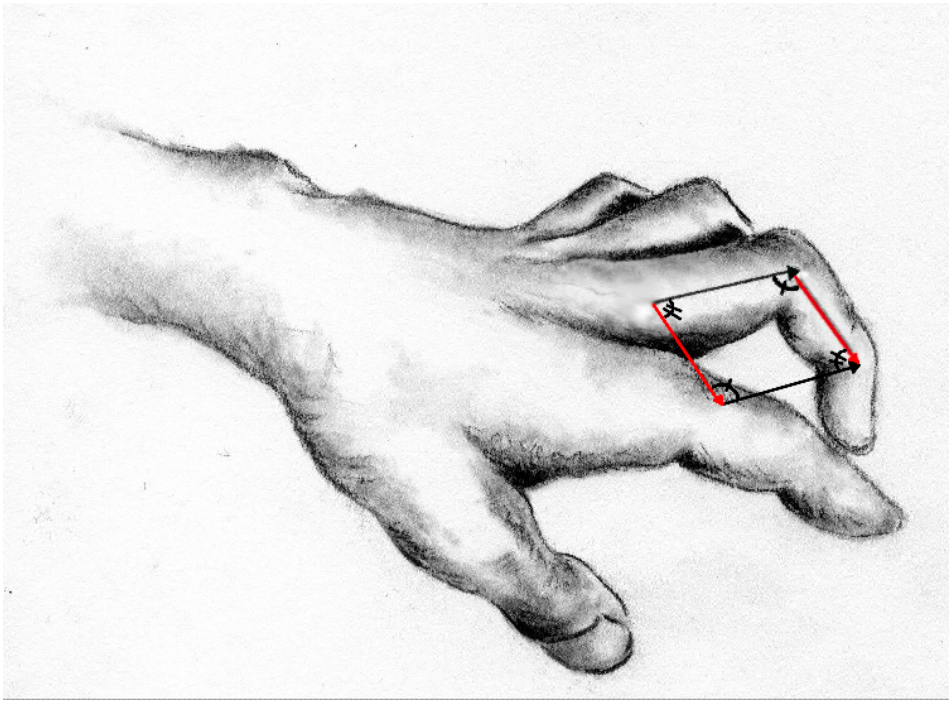

Figure 4.4: Illustration of how joint angles were mathematically obtained.

$$Angle = \frac{360° - 2 * cos^{-1}(\frac{\mathbf{v_1} \cdot \mathbf{v_2}}{|\mathbf{v_1}||\mathbf{v_2}|})}{2} \tag{4.2}$$

The 17 chosen features (listed in table 4.1 and visualised in figure 4.5) were used and the rest of the tracking information from the Leap Motion controller was discarded.

Feature nr.	Description
1	Pitch
2	Roll
3	Yaw
4-7	Angle between fingers
8-17	MP and PIP joint angles

Table 4.1: Description of features. All features are angles measured in degrees.

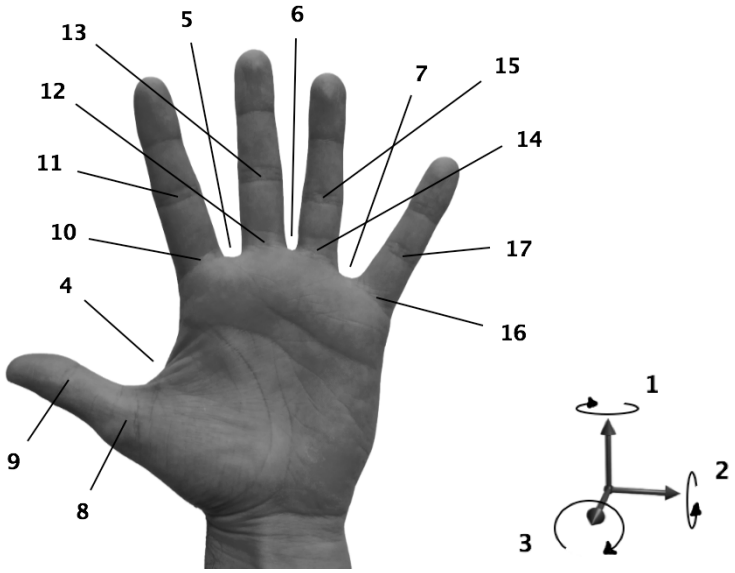

Figure 4.5: Illustration of numeral designations of features.

Step 5 - Calculate angular correlation coefficients and create correlation matrices/plots

Matrices with feature information from all repeats were created for each sample. Since each movement was repeated 100 times, 100 angular values were obtained from each sample of the movements. The matrices were used to calculate and plot the pair wise correlations using the corrcoeff-command. This way, all correlations between the 17 angle features were obtained for each sample. The correlation values, being within the span of r=0 (no correlation) to r=1 (full correlation), were plotted in a greyscale matrix plot where 0 correlation would show as white and full correlation would show as black. The correlation coefficients were then plotted over time to see how they changed during a movement.

Step 6 - Perform PCA

PCA was performed for each sample point on the matrices with feature information from all repeats using the princomp-command. Eigenvalues of each principal component were obtained, and a percentage of the total variance that each principal component accounts for was calculated by dividing the eigenvalue of said principal component with the sum of all eigenvalues. The results of the PCA were evaluated to corroborate that dimensionality reduction was possible and appropriate for future studies.

4.4.2 EEG

The flow chart in figure 4.6 gives an overview of the data processing performed on data from the EEG system during the simultaneous data collection described in section 4.3. Processing in this section is dependant on results from the previous section (4.4.1).

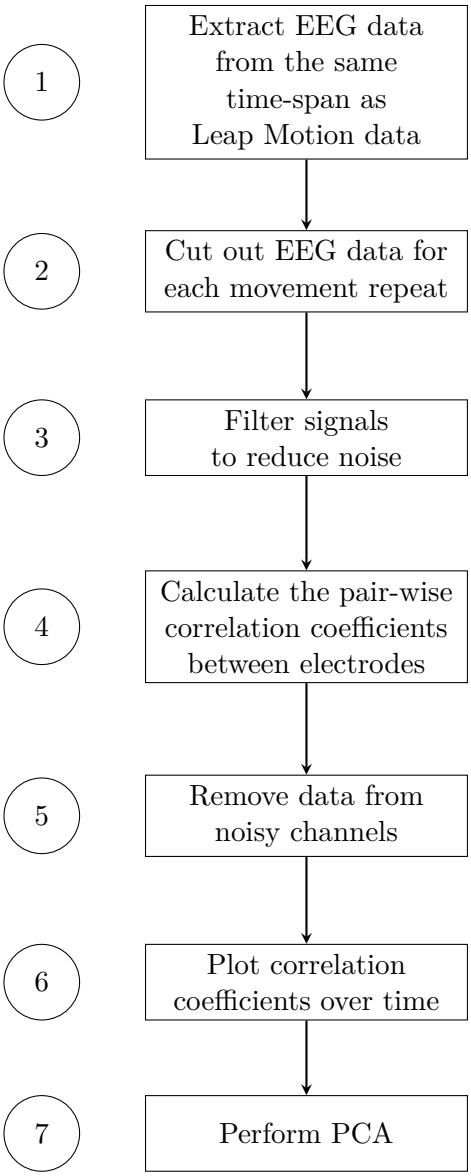

Figure 4.6: Flow chart of EEG data processing.

Step 1 - Extract EEG data from the same time-span as Leap Motion data

The collected raw data files of the EEG recordings during the four reach-to-grasp movements by each subject were obtained in the form of large matrices with all 128 electrodes represented row-wise. The measured electrode amplitudes in each sample were represented column-wise. The matrices of each subject were loaded into MatLab. The sample numbers from the initial and terminal marks created in the EEG recordings (described in section 4.3) were used to find the beginning and the end of each session. Everything outside of that time span was removed so that the EEG and Leap Motion data files were matched time-wise. Furthermore, the row representing the ground electrode was removed form the data matrix.

Step 2 - Cut out EEG data for each movement repeat

Since the two systems had different sampling rates, the starting sample numbers from the Leap Motion recording as well as the number of samples a repeat consisted of needed to be translated from Leap Motion samples to EEG samples. To do this, the vector of Leap Motion starting point samples was scaled appropriately by dividing each point with the total amount of Leap Motion samples and then multiplying them with the total amount of EEG samples. This stretched the vector of Leap Motion starting sample points to fit the EEG data. The new sample vector was used to cut out the EEG data belonging to the movements cut out from the Leap motion data as described in section 4.4.1.

Step 3 - Filter signals to reduce noise

Mean amplitudes of all repetitions for each electrode were created and visualised to screen for reoccurring patterns within recordings from each individual electrode as well as between different electrodes. Additionally, this was also used as an initial approach to identify noisy electrodes that would likely distort the results when proceeding with further analysis, and might therefore need to be removed during future processing. The number of each of the identified noisy electrodes were written down. All EEG data was filtered using a Savitzky-Golay filter (command sgolay in MatLab) in order to reduce high frequency noise. Various filters were available in MATLAB and the results obtained by using a number of different filter types, orders and coefficients were examined evaluated by observing the plots before and after filtering.

Step 4 - Calculate the pair-wise correlation coefficients between electrodes

For each sample during the movements, a matrix with electrode information from all repeats during that specific sample was created. Thus, since each movement was repeated 100 times, 100 amplitude values from each of the 128 electrodes were obtained for each sample of the movements. This information was used to calculate and plot the pairwise correlations using the corrcoeff-command. Greyscale correlation matrices spanning from r=0 (no correlation, white colour) to r=1 (full correlation, black colour), were plotted for specific points in time, namely the start, middle and end point of each movement. To be able to examine the changes in correlation coefficients over time, these calculations were expanded to cover all sample points.

Step 5 - Remove data from noisy channels

In the grey-scale correlation matrices, highly noisy channels were identified by their consistently dominating white colours, corresponding to low correlation with all other electrodes and therefore interpreted as noise. The numbering of these electrodes were checked against the list made during step 3 to confirm that this interpretation was correct. Thereafter, data from the noisy channels were removed from the correlation matrices.

Step 6 - Plot correlation coefficients over time

After removing the noisy electrodes, the correlation coefficients were once again plotted over time to see how they changed during a movement as for the Leap Motion data in section 4.4.1, step 5. The process of creating these plots were fairly similar, the largest difference being the number of correlation coefficients. Whereas the the number of correlation coefficients for the Leap Motion data was 136 the number for the EEG data was closer to 15,000.

Step 7 - Perform PCA

PCA was performed on the matrices representing each sample point with information from all repeats and all remaining electrodes using the princomp-command. Eigenvalues of each principal component were obtained, and a percentage of the total variance that each principal component accounts for was calculated by dividing the eigenvalue of said principal component with the sum of all eigenvalues. The results of the PCA were evaluated to corroborate that dimensionality reduction was feasible and appropriate for future studies.

4.5 Matching Leap Motion and EEG data

One of the aims when proceeding further with this study is to match the Leap Motion and EEG correlation coefficient data (as shown in chapter 5, figure 5.25). These plots from the different subjects were visualised and compared to analyse how they should be treated in future studies to find underlying information. Methods of identifying specific synergies in the Leap Motion data and matching them with the possible synergies in the EEG data were reflected upon and considered for the future.

Chapter 5

Results

The following list is a brief summary in text of the results obtained for each goal.

- Initial analysis of test data
  - Obtained finger tip coordinate plots show that glitches in Leap Motion data could be minimised by keeping the hand inside the controller field of view at all times during recordings. Visualisation of coordinate data from Leap Motion showed that movement repeats were possible to identify and extract by finding the initiations of the reach-to-grasp movements in the finger tip coordinates. Plotting recorded angle data against each other during repeats of different movement types revealed both that correlations between several angles exist and that the movement types are distinguishable in the data, indicating that varying reach-to-grasp movement types are separable through their data and that correlation analysis is a useful tool for upcoming data analysis.
- Design of reach-to-grasp movements
  - Four different types of reach-to-grasp movements were selected.
- Simultaneous collection of Leap Motion and EEG data
  - Since all four test subjects repeated four different movement types approximately 100 times each, four Leap Motion recordings and four EEG recordings were collected from each subject, resulting in a total of 16 Leap Motion data files and 16 EEG data files.
- Separate data analysis
  - Leap Motion: As in the results of the initial analysis of test data, correlation matrices for fixed time values were obtained from the Leap

Motion data. In addition to this, the same type of matrices in a grey-scale representation of correlation value were obtained for improved visualisation and an overview of correlations between angles of the hand. Plots of angular correlation values during the entire course of the movements were obtained for an overview of how the angle correlations vary in time, showing groups of similarly behaving correlation patterns, indicating synergies. PCA analysis showed initial principal components with high eigenvalues, indicating possibility of reduced dimensionality and thereby also the possibility of synergies.

  - EEG: Initial visualisation of mean electrode amplitudes during movement repeats showed groups of similarly behaving electrodes. Grey-scale correlation matrices showed high correlation values between many electrodes at fixed samples. Plots of correlation values between electrodes visualised over time also showed groups of similarly behaving correlation patterns, indicating a possibility of synergies in the cortex. PCA analysis showed high eigenvalues for the first few principal components, also supporting the possibility of reduced dimensionality, possibly also the synergy theory.

- Matching Leap Motion and EEG data

  - Comparison between the obtained angular and EEG correlation coefficient plots showed how the correlation behaviour of the two data sets were related in time domain. Some methods for future data processing were suggested.

More detailed results in the form of figures, tables and descriptions are found in the titled sections ahead.

5.1 Initial analysis of test data

As mentioned in section 4.1.1, removing the hand from the Leap Motion field of vision between each repetition of a movement caused glitching. Figures 5.1 and 5.2 show xyz-coordinates of the thumb fingertip during Leap Motion testing. The glitching problem can be seen in figure 5.1, and the area around sample 8600 shows the most evident glitching. This was a recording where the hand left the controller field of view between each movement repetition. The glitching problem is minimised by keeping the hand inside the controller field of view at all times during recording, as can be seen in figure 5.2.

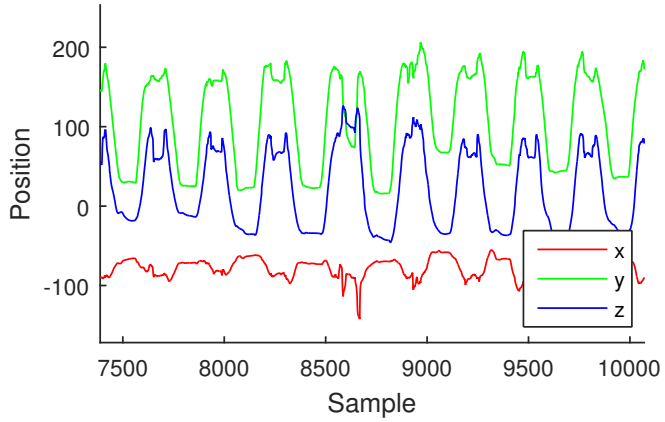

Figure 5.1: Glitching in Leap Motion recording seen in thumb fingertip coordinates.

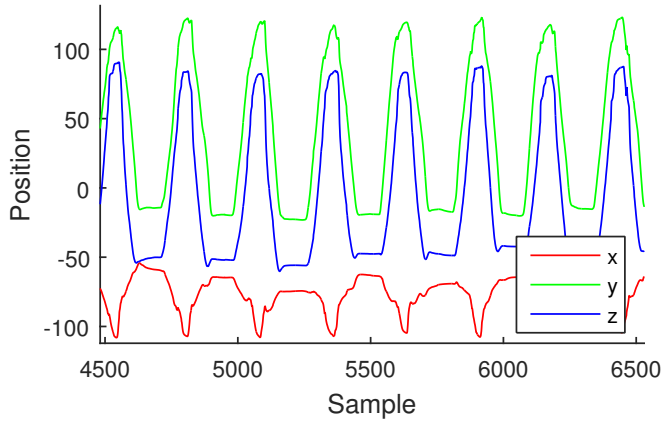

Figure 5.2: Glitching problem seen in figure 5.1 reduced by ensuring that the hand does not leaves the field of view of the Leap motion controller between the repeats of a movement.

In figure 5.3, the xyz-coordinate plot of the thumb fingertip coordinates for one movement type is zoomed in to demonstrate the appearance of the trajectories. The start point is marked by an arrow and the region where the end point (the actual grasping of the target object) is located is marked by a circle. This was the typical shape for all repetitions and movement types. As this figure shows, the starting point of each movement generates a sharp change in the curve and is therefore more distinct than the end point, which is smoother and more rounded.

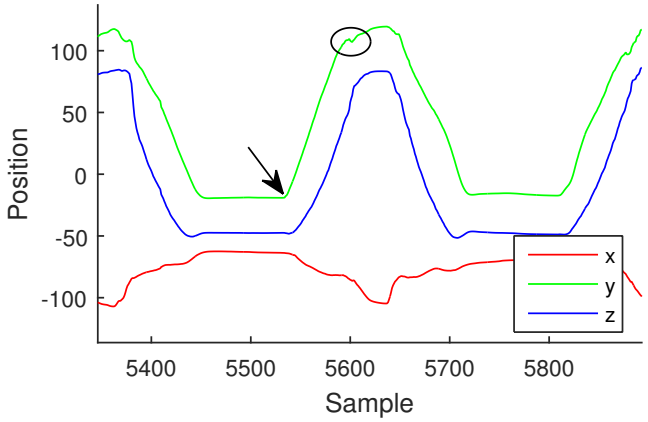

Figure 5.3: Example of what the start- and end points of a repetition typically look like for the xyz-coordinates of the thumb fingertip.

Figure 5.4 shows all 17 features (angles of the hand) at a fixed time during the 50 test repeats of three different types of test movements plotted against each other. The test movements were a precision grip of a small desk lamp, a power grip of a pen and a grasping of a round lid with all finger tips. It shows that correlations between the features (angles) exist within the different movement types. Stronger correlations related to all movement types can for example be seen in (row 15, column 11), where the data points appear in a diagonal line. This is an indication of a correlation between PIPs of the index finger and ring finger, which have the feature numbers 11 and 15, shown in figure 4.5. The correlation means that the synergistic muscle system of the hand encourages bending of both these PIP joints in synchronisation with each other during all test movements. The same phenomenon can for example be seen in (row 16, column 12) which indicates a correlation between the MPs of the middle finger and the little finger. In some cases, the areas of data points from the different movement types overlap (see for example (row 9, column 7), showing values of the thumb DIP angles plotted against the values of the angles between the ring finger and little finger). In other cases, the areas are clearly separable (see (row 3, column 2), showing yaw angles of the hand plotted against the roll angles of the hand). The cases where the areas don't overlap can be used to distinguish between different movement types, which is useful for future work. Rows/columns 5 and 6 show the angle between the index finger and middle finger, and between the middle finger and ring finger respectively, plotted against other angles. As seen in figure 5.4, these plots are examples where the data points stay within a short span on the axis. This means that the spreads of angular values of feature 5 and 6 are small, meaning that the

angles between said fingers are somewhat constant for these specific movement types.

The most important overall information obtained from the plot in figure 5.4 is that correlations between hand angles are present for some angle pairs (data points appearing in a diagonal line) and absent for some (no visible diagonal appearance), areas of data points from different movement types overlap in some plots and not in others, etc. The high variation of how the data points appear in the plots provides a basis with both unique features and features in common for different movement types, pointing towards the ability of separating and identifying movement types, as well as visualising a muscle synergy basis for future work.

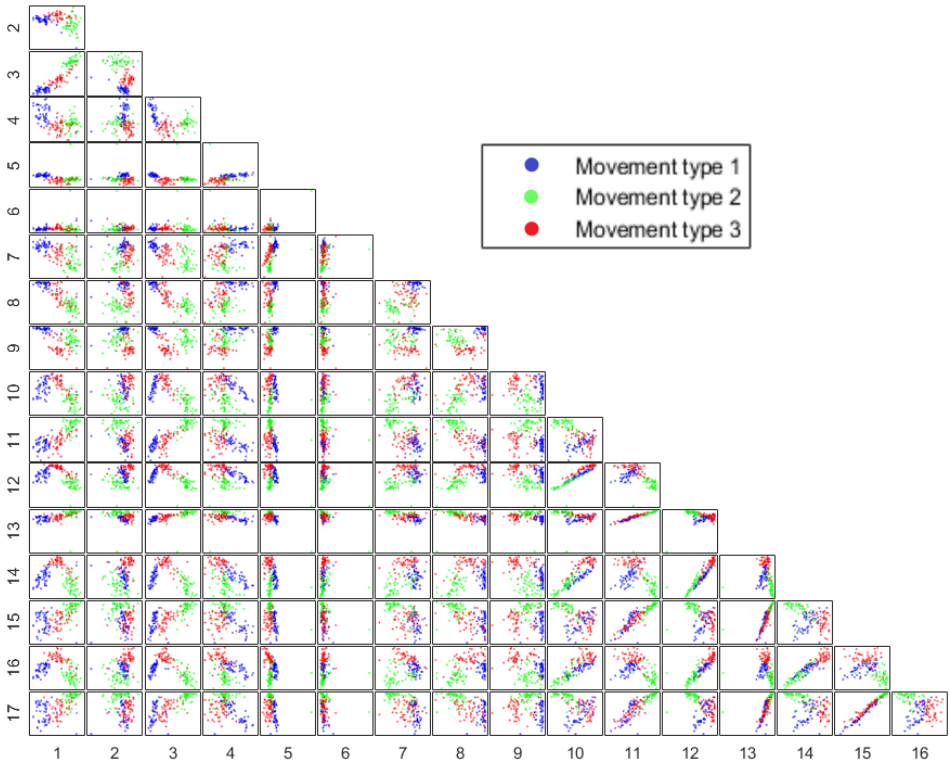

Figure 5.4: Scatter plot matrix for 50 repetitions of three different types of test movements.

5.2 Design of reach-to-grasp movements

The four definitive reach-to-grasp movements chosen for analysis were a power grip of a pen, an angled power grip of a pen, a precision grip of a pen and a wide grasp of a bottle as shown in figure 5.5. The figures illustrate the terminal grasps of the movements. The reaching motion prior to grasping is performed in a straight-forward trajectory with the hand inside the Leap Motion controller field of view at all times. The arm is relaxed on a pillow between each iteration of the movements.

(a) Wide grasp.

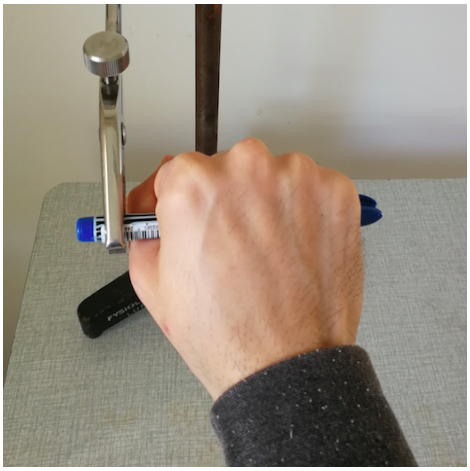

(b) Power grip.

(c) Angled power grip.

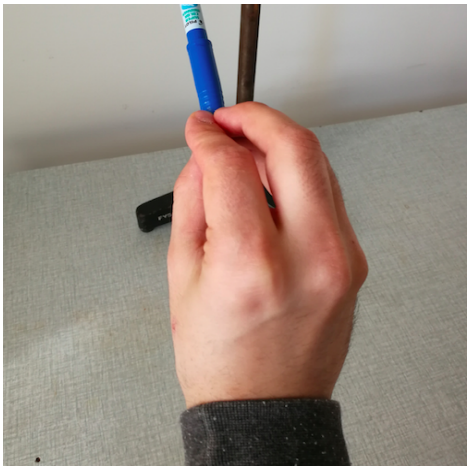

(d) Precision grip.

Figure 5.5: Terminal grasps of the four selected movements.

5.3 Simultaneous collection of Leap Motion and EEG data

The simultaneous data collection for each subject resulted in four .dat files containing Leap motion recordings of all positional tracking data shown in figure 3.3 along with roll, pitch, yaw and bone vectors for the different movement types, as well as four .mat files with corresponding EEG amplitude recordings in the 128 electrodes. Additionally, the EEG data files included additional information such as sample rate as well as markers representing the start and end of each recording session.

5.4 Separate data analysis

All plots displayed from this point and forward in the report are created with data from one representative subject.

5.4.1 Leap Motion

Figure 5.6 shows a matrix where each small plot shows data points of one specific angle plotted against another specific angle from 100 repeats of each movement type at a fixed point in time. The displayed time point is the mean of the last 10 samples of each movement repeat. The angles can be numerically identified on the axes and thereafter anatomically identified through figure 4.5. The concept is the same for the test plots in figure 5.4. The matrix shows that the four movement types are separable when plotting data points from some angles against each other. A clear example of this is for example all boxes in column 2 that show the data points of the roll of the hand plotted against all other tracked angles. In most of these boxes, and especially for the case in row 4, column 2 which shows the data points of the roll of the hand plotted against the angle between the thumb and index finger, the data points of the four movement types are separated into their own regions. This information is valuable since it is important to be able to separate movement types in the data for future synergy identification. In some plots the regions overlap, for example row 8, column 7 shown in figure 5.7. The plots in rows and columns 10-17 show data points of the MP and PIP joint angles plotted against each other. Most of the data points in these appear in a diagonal line, indicating a correlation between MP and PIP joint angles which is consistent for all four movements. A clear example of this is shown in figure 5.8. Correlation between angles in the hand is an indication that muscles acting on those joints work together to create a movement as a whole - in other words a muscular synergy.

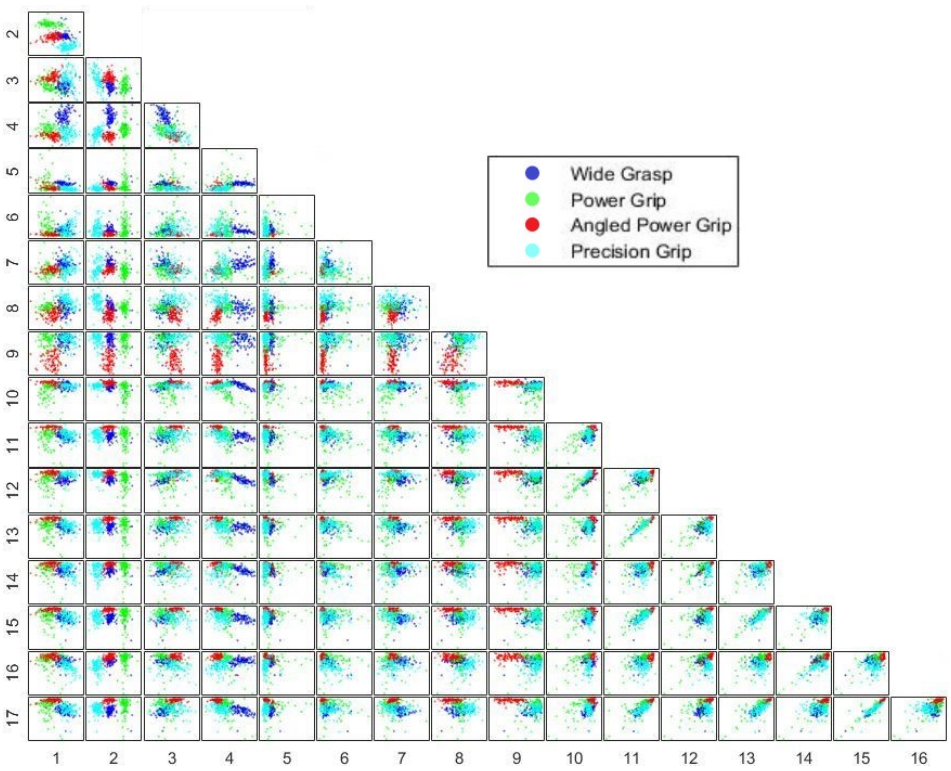

Figure 5.6: Scatter plot matrix of recorded Leap Motion angles at the end of all four hand movements.

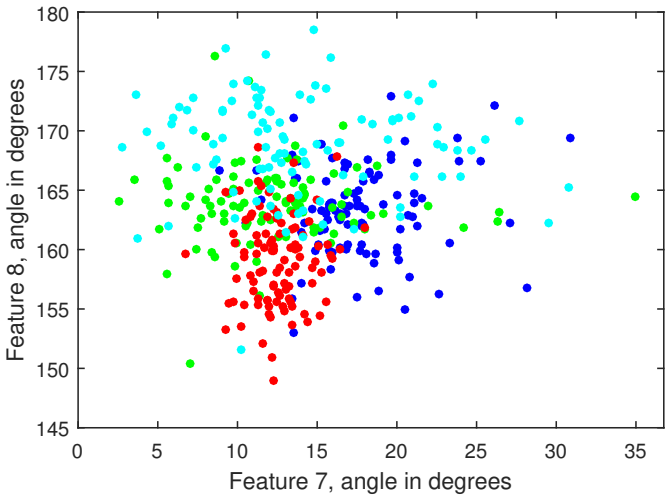

Figure 5.7: Row 8, column 7 from figure 5.6 zoomed in.

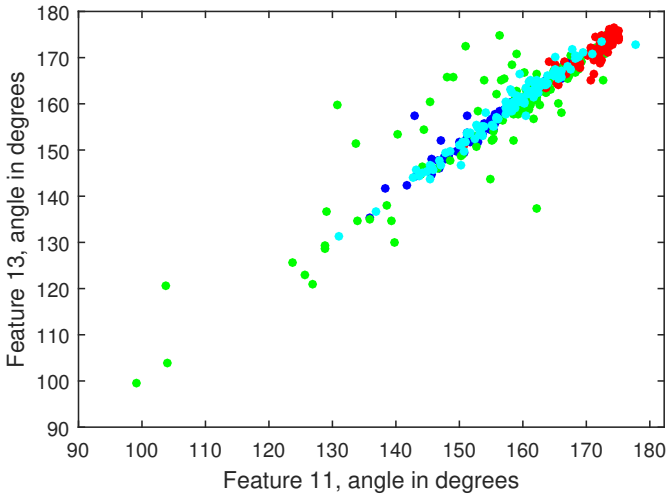

Figure 5.8: Row 13, column 11 from figure 5.6 zoomed in.

Since the type of angular plot in figure 5.6 does not quantify the correlation, correlation values extracted from the plot during the start, middle and end of all four hand movements are plotted in figure 5.9 in a grey-scale representation. Each pixel represents a correlation value between two angles where black indicates a high correlation and white indicates a low correlation. The figure shows that there are collective components with similar correlation behaviour within each movement at different points in time. For example, the plots in rows and columns 10-17 that remain black throughout the movements indicate a high correlation and thereby the presence of muscular synergies throughout the movement. There are also uniquely behaving correlations present within each movement at different points in time, for example row 3, column 1 for the power grip showing the correlation coefficient for the yaw angles against pitch angles. It starts out with a high correlation but decreases throughout the movement. These types of unique movement-dependent angular correlations are important for future connection to movement-dependent EEG electrode correlations for synergy analysis.

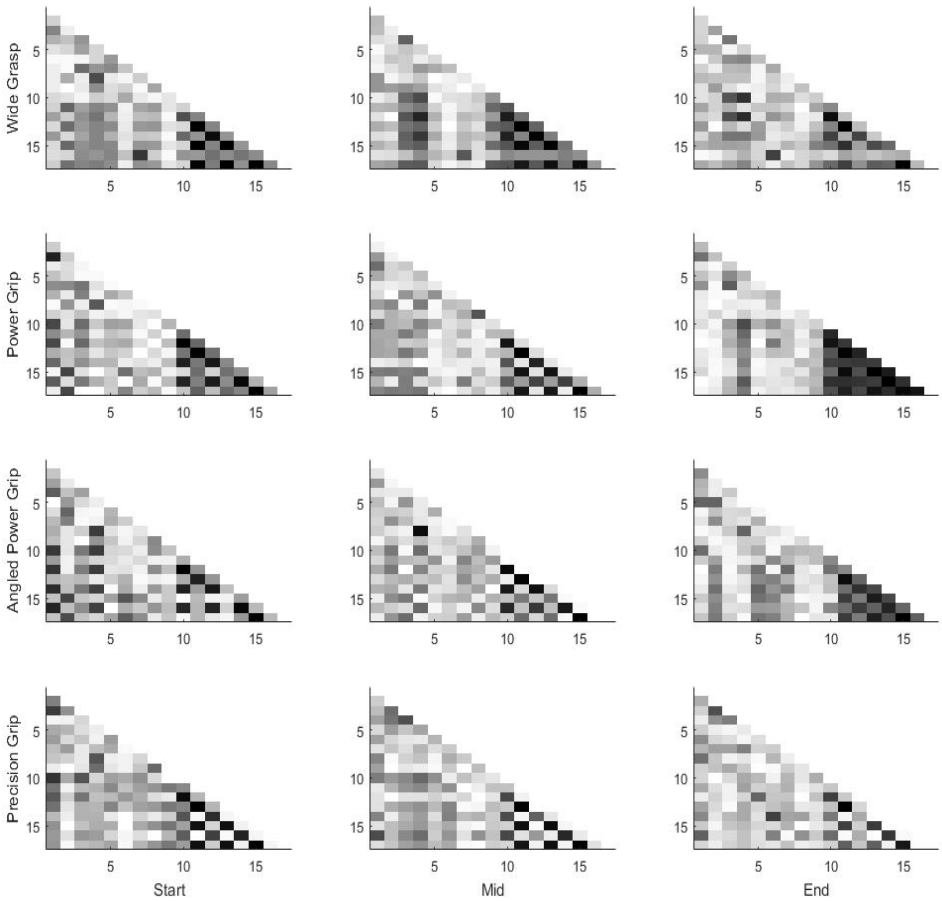

Figure 5.9: Correlation coefficients of recorded Leap Motion angles during start, middle and end of all four hand movements. Black corresponds to a correlation of 1 (100%) and white to a correlation of 0 (0%).

A detailed plot of how each correlation coefficient in the movement matrices changes throughout the time-line of each movement can be found in figures 5.10-5.13. In these plots, there are a total of 136 correlation coefficients representing correlation values between the angles of the hand, each represented by a line. Many of the lines have adjacent lines which are behaving similarly to them, indicating similarly behaving correlation patterns between different angles of the hand. This indicates several pairs of joints correlating in a similar manner, pointing towards patterns of muscular synergies acting uniquely during each movement type. These specific patterns need further exploration and comparison with EEG patterns to reach full potential.

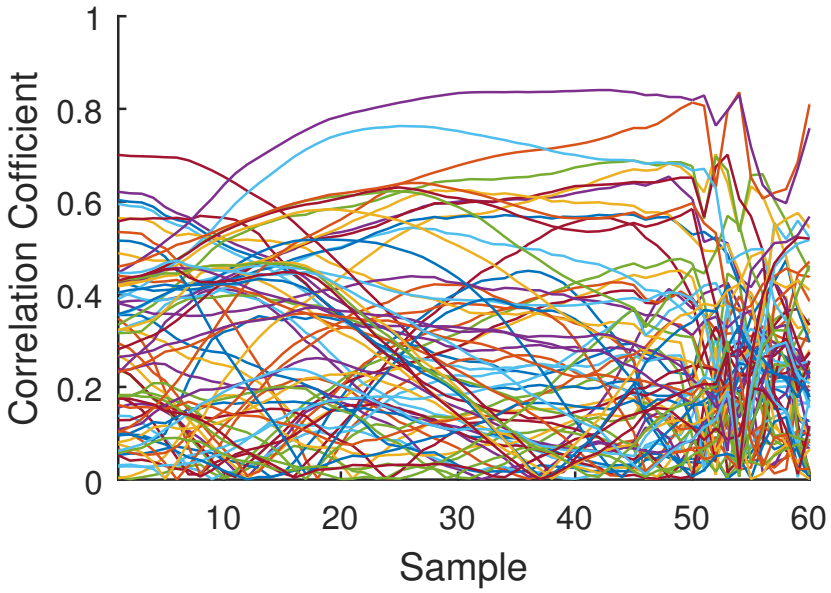

Figure 5.10: Correlation coefficient time-line for the wide grasp movement type.

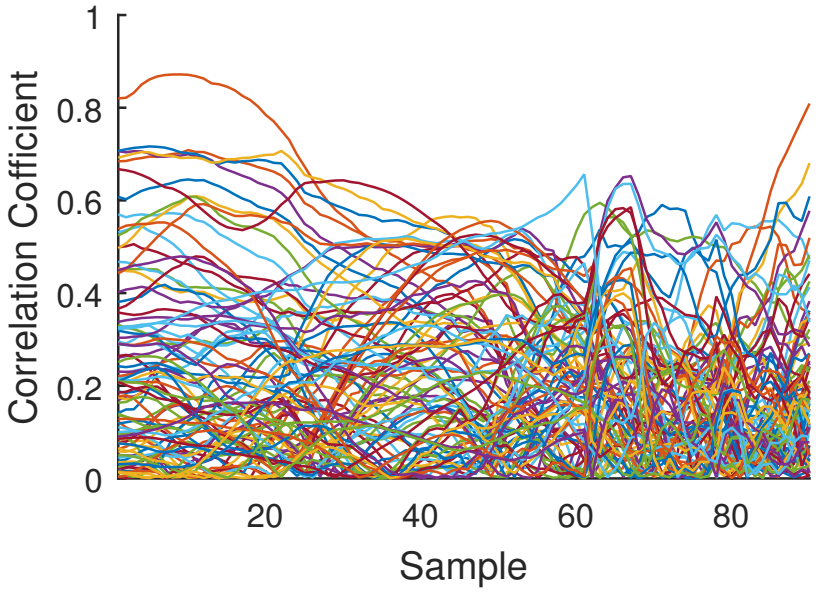

Figure 5.11: Correlation coefficient time-line for the power grip movement type.

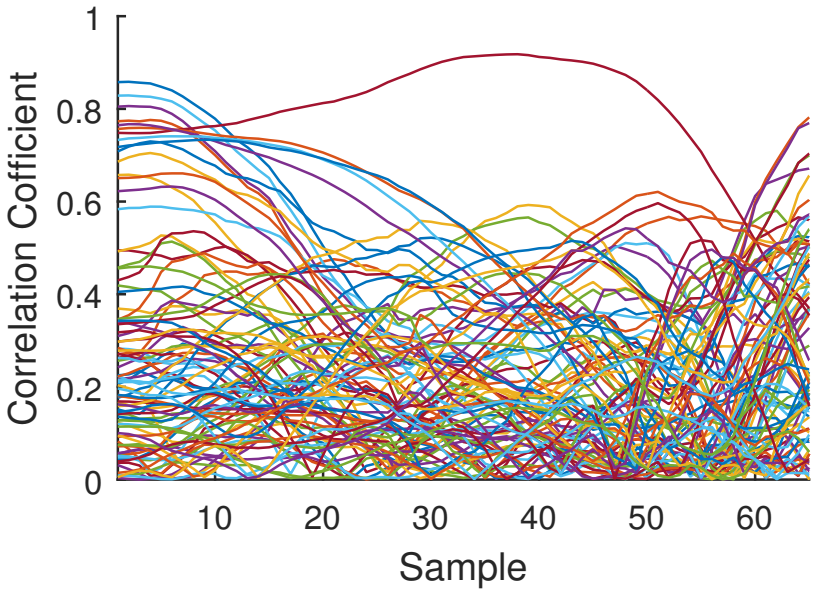

Figure 5.12: Correlation coefficient time-line for the angled power grip movement type.

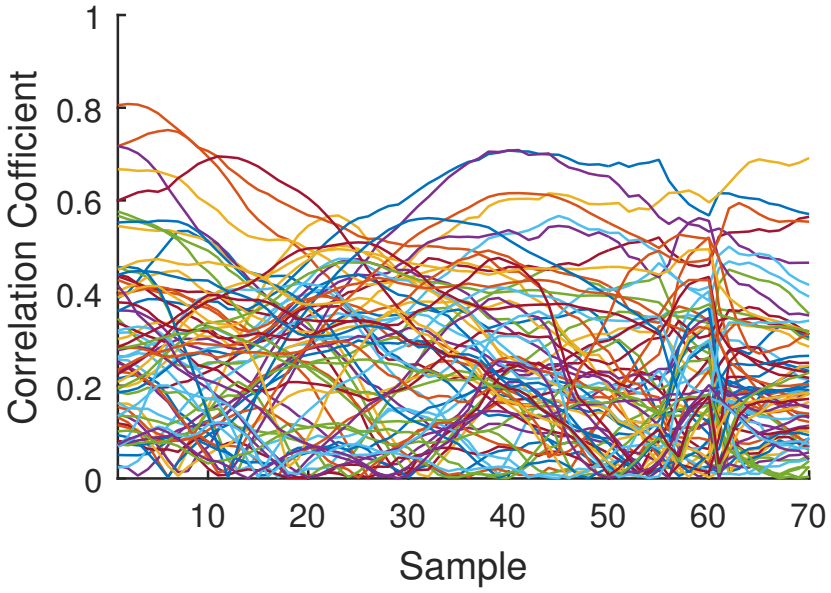

Figure 5.13: Correlation coefficient time-line for the precision grip movement type.

The results of the PCA performed on Leap Motion data can be seen in table 5.1. The PC's are represented as the percentage of the total variance that they account for. The values confirm that a substantial reduction of the dimensionality is possible while still giving a sufficient description of the movement trajectories, which is a feature that appears when synergy is present.

	Wide grasp	Power grip	Angled power grip	Precision grip
PC_1	46.96	48.16	45.31	34.94
PC_2	17.70	17.31	17.74	26.65
PC_3	10.52	10.93	11.94	10.80
PC_4	6.66	7.03	6.07	7.94
PC_5	5.05	4.70	5.31	5.37

Table 5.1: Percentage of variance accounted for by each principal component (mean of each trajectory) for Leap Motion data.

5.4.2 EEG

As mentioned in sections 4.1.2 and 4.4.2, events in the Leap Motion data that were interpreted as the start of a movement were manually selected and used to cut out both the Leap Motion and EEG data of each movement. Figure 5.14 shows the result of the matching between Leap Motion and EEG data.

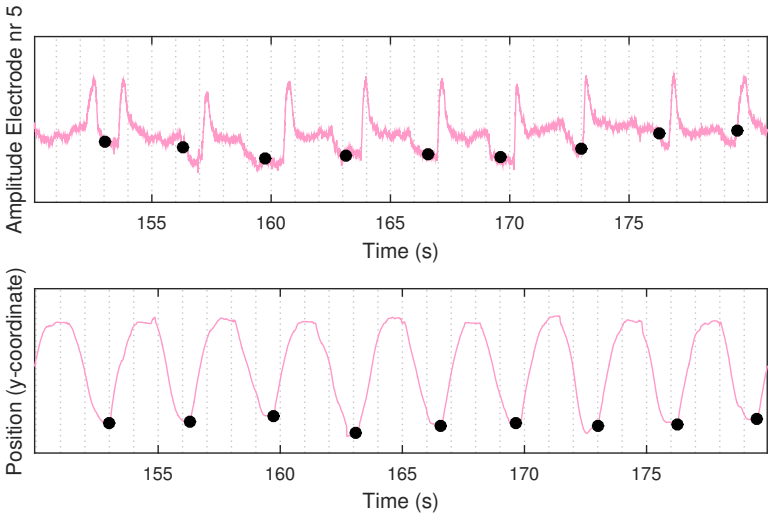

Figure 5.14: Matching of time-line events between Leap Motion and EEG data.

Figures 5.15 and 5.16 are representations of the signal to noise ratio in all electrodes at a specific point in time (sample 200). The figures shows a high spread of recorded amplitudes of all wide grasp movement repeats at the fixed time. The black markings show the mean recorded amplitude in the electrodes.

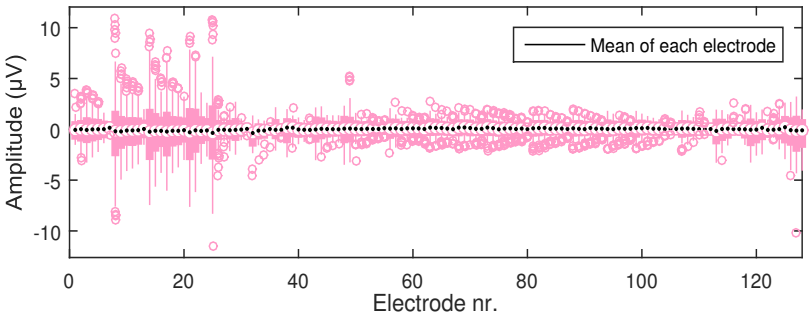

Figure 5.15: Box plots of smoothed data in all 128 electrodes at a fixed time (sample 200).

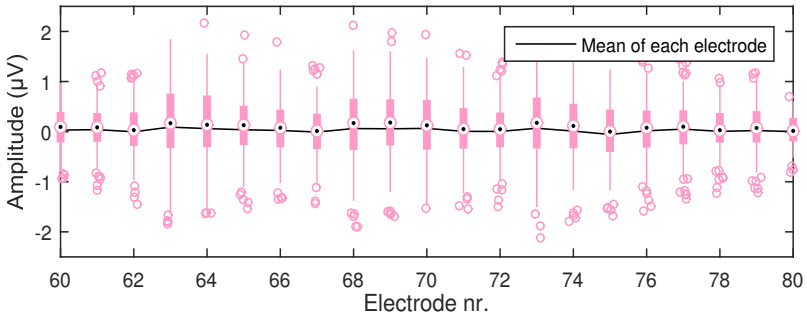

Figure 5.16: Figure 5.15 zoomed in.

Figures 5.17-5.20 show the mean EEG amplitude curves (raw and smoothed with filter) in different electrodes from all repetitions of the wide grasp movement. Mean EEG amplitudes in figures 5.17 and 5.18 show behaviours similar to each other. The same goes for the amplitudes in figures 5.19 and 5.20. The electrodes showing similar behaviours are located in proximity to each other. The illustrated mean amplitude values show that there are different dominant activities during the course of a hand movement in different areas of the cortex.

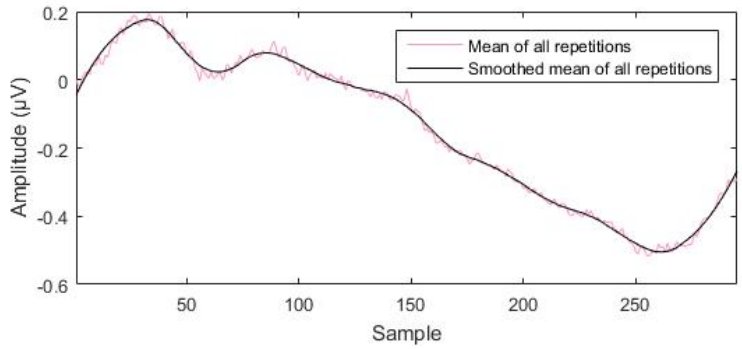

Figure 5.17: Mean EEG amplitude curve of all wide grasp repetitions in electrode 2.

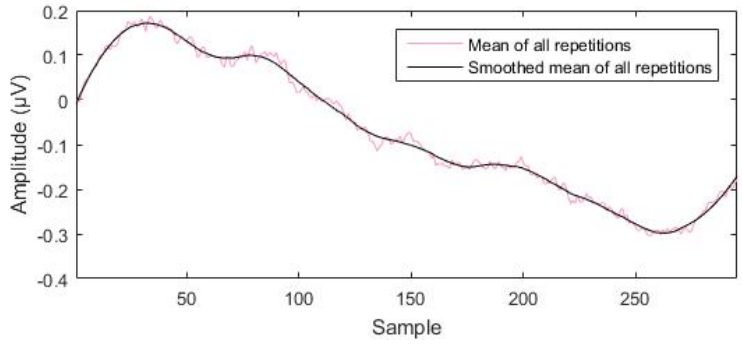

Figure 5.18: Mean EEG amplitude curve of all wide grasp repetitions in electrode 27.

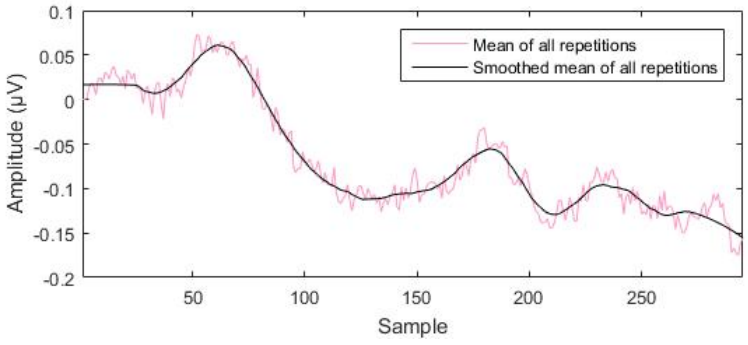

Figure 5.19: Mean EEG amplitude curve of all wide grasp repetitions in electrode 44.

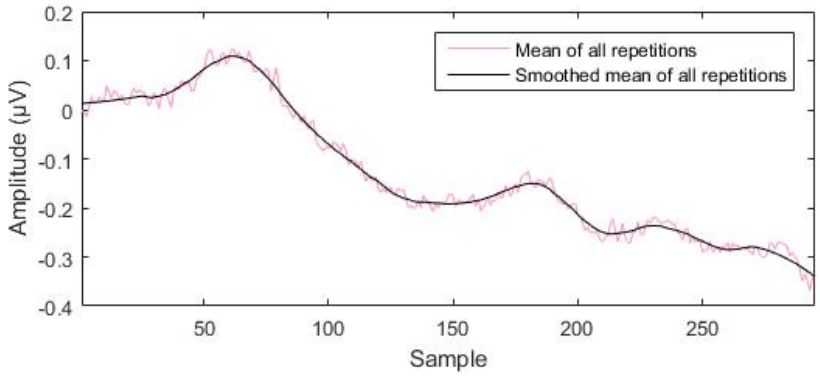

Figure 5.20: Mean EEG amplitude curve of all wide grasp repetitions in electrode 128.

Figure 5.21 shows the mean EEG amplitude curve from the same subject in electrode 68. There is substantial visible noise in this electrode.

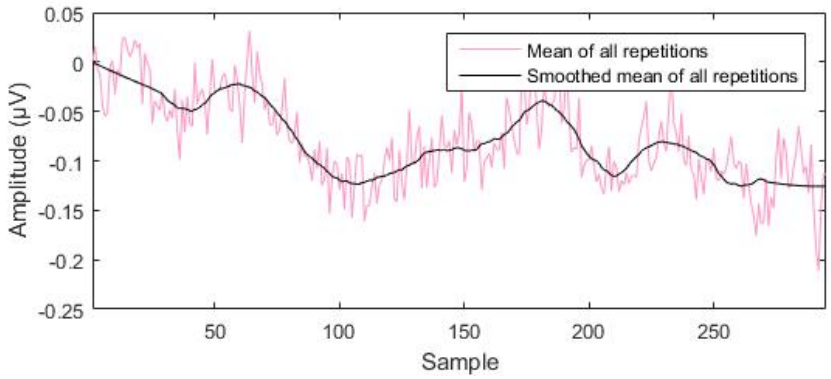

Figure 5.21: Mean EEG amplitude curve of all wide grasp repetitions in electrode 68.

Figure 5.22 shows a correlation coefficient matrix from sample 200 with all 128 EEG electrodes as features. This matrix is created with calculated EEG correlation data in the same manner as the matrices in figure 5.9, although each pixel here shows the correlation between two electrode amplitudes instead of two angles.

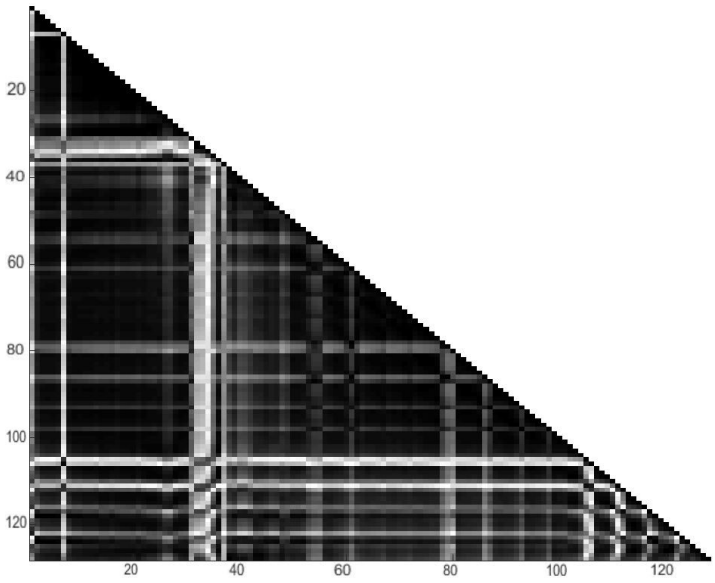

Figure 5.22: Correlation matrix from sample 200 of the wide grasp movements.

Since the white lines in figure 5.22 reflect low correlation and thereby deviant behaviour, they are interpreted as noisy channels. The result of removing these electrodes can be seen in figure 5.23.

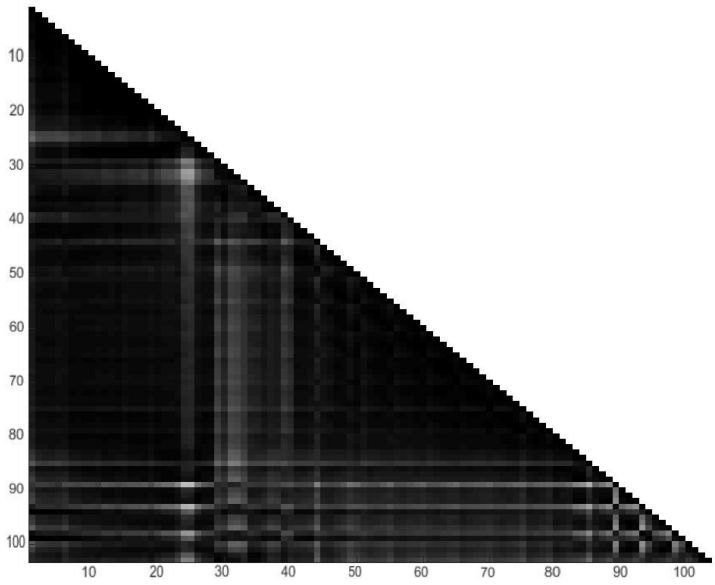

Figure 5.23: Figure 5.22 with noisy electrodes removed.

A plot showing how each EEG correlation coefficient from the matrix in figure 5.23 changes throughout the time-line of the precision grip movement can be found in figure 5.24. As seen for the Leap Motion data in figures 5.10-5.13, many of the lines in figure 5.24 have groups of adjacent lines behaving similar to them, indicating similarly behaving correlation pattern between different groups of electrodes. This is an indication of synergies in the cortical activity.

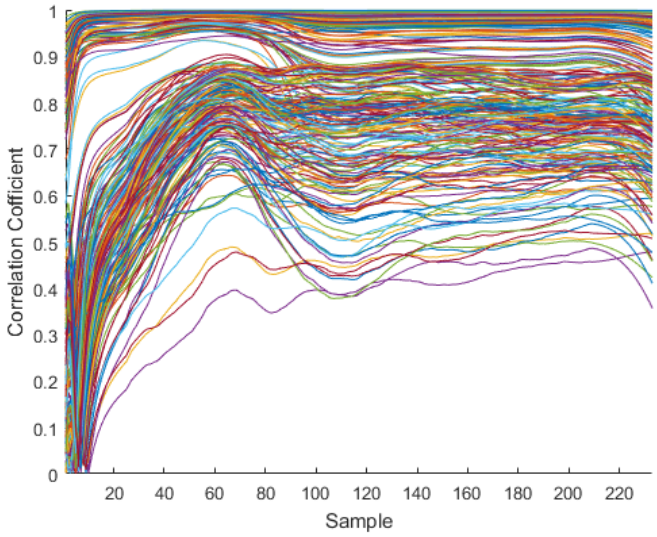

Figure 5.24: Changes in correlation coefficients for EEG data during precision grip movements.

The results of the PCA performed on the EEG data can be seen in table 5.2. The high values of the first few PC's indicate that a substantial reduction of the dimensionality is possible while still describing a large part of the activity in the cortex, supporting cooperation and synergistic behaviour in the CNS.

	Wide grasp	Power grip	Angled Power grip	Precision grip
PC_1	86.40	76.37	78.62	87.09
PC_2	5.88	12.05	11.03	6.04
PC_3	3.93	4.24	3.93	2.40
PC_4	1.20	1.83	1.77	1.05
PC_5	0.49	1.12	1.18	0.70

Table 5.2: Percentage of variance accounted for by each principal component (mean of each trajectory) for EEG data.

5.5 Matching Leap Motion and EEG data

Figure 5.25 shows an example of how the changes of correlation coefficients from the Leap Motion and EEG data are related in the time domain.

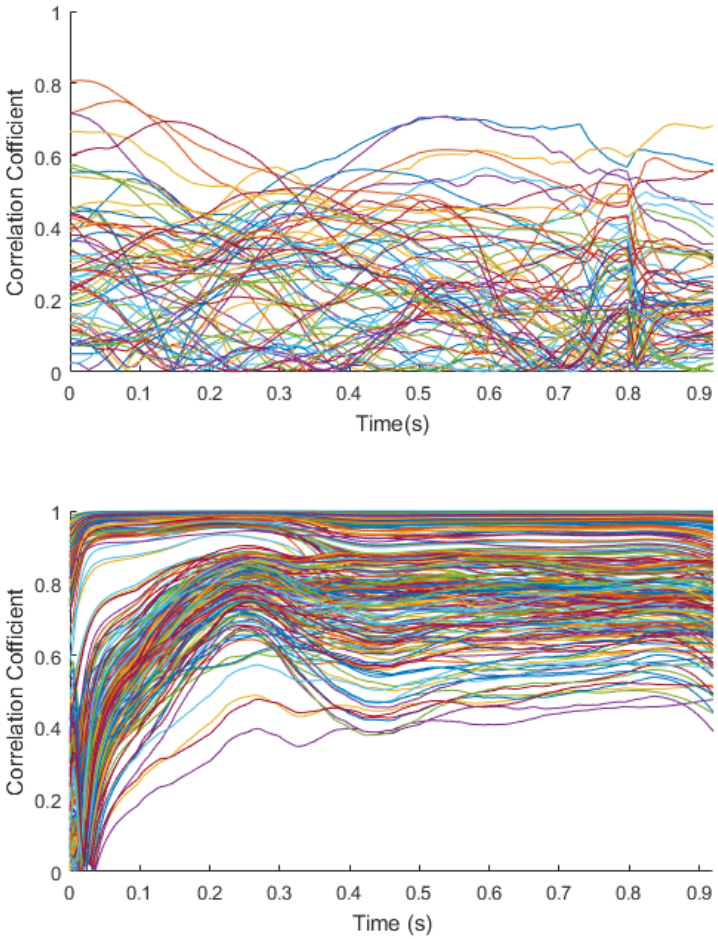

Figure 5.25: Correlation coefficients from the Leap Motion device (top) and EEG recording (bottom) for the precision grip.

Figure 5.25 clearly shows that due to the number of lines in the plots, further data processing and parameter reduction needs to be applied before any definitive conclusions can be reached from the data. By applying time continuous dimensionality reduction (PCA) to the correlation coefficient data, an interpretation of whether synergies at the joint/muscular level are mirrored by the activity distribution in the brain could be obtained. This may be the planned course of action for the future.

Chapter 6

Discussion and Conclusions

6.1 Leap Motion

The mixture of reoccurring and differing correlation values within and between movement types seen in figure 5.9 is what we set out to find in the Leap Motion data. It provides a wide basis for future work. Additionally, the first five principal components from the PCA account for approximately $86 - 88\%$ of the movement, serving as further support of the possibility of dimensionality reduction and muscle synergies. As a whole, the results from the Leap Motion data analysis indicate synergistic behaviour between angles (and thereby also muscles) of the hand, which was expected considering that muscular synergies are documented. In conclusion, the analysis of the Leap Motion data has at this point served two main purposes among others: confirmation of documented muscle synergies in the hand (indicating a correct path of analysis), and providing an important tool for the search and identification of specific synergies in the CNS through data processing and comparison with recorded EEG signals.

6.2 EEG

Figure 5.14, which illustrates the temporal matching of EEG and Leap Motion data, shows clear reoccurring patterns and similar data behaviour between each event in the two data types. This is interpreted as a sign of successful temporal matching between EEG and Leap Motion data, which is critical for obtaining coherent and relevant EEG data during the movement repetitions.

Figure 5.21 illustrates the high level of noise seen in electrode number 68. This kind of noisy electrodes are an inevitable part of the EEG since some of the electrodes may lose contact with the scalp and some are attached in proximity to

muscles controlling for instance the eyes, neck and jaw, producing mostly noise. High noise levels are important to handle appropriately since they disturb data and interfere with analysis. Noise was handled by filtering the data and thereby creating the smoothed black lines seen in the EEG plots. Electrodes with exceptionally high levels of noise such as electrode 68 were removed completely from the data to stop them from interfering with further analysis.

Strategies of removing the noisy channels (such as visualising the average data in all electrodes) were discussed during the course of the analysis. Many discussed strategies were time consuming. By creating a correlation matrix from the EEG data, a simple solution to this problem was found. Figure 5.22 shows the correlation matrix of the EEG data from the wide grasp movements. In this figure, white lines are visible. A high level of noise suppresses the underlying signal and should as a result reduce similarity of patterns between electrodes. Therefore, the white lines are interpreted as very noisy electrodes since they correspond to low correlation between the numbered electrode and all other electrodes. Identifying the noisy electrodes in this way and removing the data from them left us with data free from large noise levels in an easy way. Figure 5.23 shows the correlation matrix free from data collected in the noisy electrodes.

Figures 5.15 and 5.16 are an analysis of signal to noise ratio. Looking at the mean amplitude values (the black markings) in the plots, they are in some electrodes very low in comparison to the span of recorded amplitudes during the movement repeats. This indicates a low signal to noise ratio which could be improved with a better EEG system. This also gave an overview of which electrodes were the most noisy ones.

As detected in the Leap Motion data, figure 5.24 shows that some correlation coefficients behave similar to each other. This, together with the high eigenvalues obtained in the first few PC's from the EEG PCA, might in the same manner as described in section 6.1 be supportive of a dimensionality reduction possibility, and the theory of a synergistic system in the CNS, which is what we hoped to find.

6.3 Sources of errors and suggested improvements

There are some sources of error that need to be addressed to validate the work in this thesis.

With our manual time-stamp method of synchronising Leap Motion and EEG data, there is an inevitable factor of human error. Despite this, since the error stays within a smaller range of milliseconds, the data sets appear to match sufficiently well to study joint events. An improved method (preferably automated) to identify

the temporal start and end of a motion would be useful for future work.

After segmentation, the collected EEG signals were filtered using a Savitzky-Golay filter before any other data processing. This filter was chosen due to its ability to minimise the temporal shift of the signal while at the same time creating an easily adjustable level of smoothing. The level of smoothing was chosen roughly by looking at the effects of the filter on data plots, which naturally contains an underlying source of human error. This could be optimised before proceeding with future data analysis.

The EEG system used for this work showed a high level of baseline drift and differences between electrode amplitudes. The data was processed accordingly during the work to minimise the negative effects of the EEG system shortages. A more reliable EEG system is recommended since it could possibly provide more stable data for future recordings.

In figures 5.10-5.13, the correlation coefficients between the angles become chaotic at certain sample points. Even if it is most probably a result of terminal glitching in the Leap Motion system, it could also be a smoothing artefact or faulty data processing. In the same manner we see a possible artefact in the beginning of the EEG correlation plot in figure 5.24. It shows an unexpected trend of low correlations in the very beginning of the hand movement. This is possibly a data processing artefact that was not addressed during the given time limit. Nevertheless, in spite of these possible artefacts the data in the plots are sufficient for serving as a basis for future work.

6.4 Future work

Through this work we have established that there is a possibility of underlying neural synergies acting on motor output during reach-to-grasp movements. However, more work needs to be done in order to validate the findings. The work in this thesis will be continued by the department of Neural Basis of Sensorimotor Control at BMC, Lund. More Leap Motion and EEG data needs to be collected, data processing needs to be improved and new methods of analysis need to be introduced and applied to the data. It is mainly the type of correlation coefficient data illustrated in figures 5.10-5.13 and 5.24 that need further clarification. There is much to explore in the Leap Motion and EEG correlation coefficient data, both on an independent level and combined. So far we have only been able to look at PCA of the data at fixed moments in time. The data needs temporal PCA analysis that clarifies the relationship between the landscapes of cortical activity and motor synergies of reach-to-grasp activity over time.

References

[1] G. Zappala, M. de Schotten, P. Eslinger, "Traumatic brain injury and the frontal lobes: What can we gain with diffusion tensor imaging?", *ScienceDirect*, 2012

[2] C. Grefkes, N. Ward, "Cortical reorganization after stroke", *The Neuroscientist*, 2013

[3] C. Taylor, R. Schwarz, "The Anatomy and Mechanics of the Human Hand", *Artificial Limbs*, 1955

[4] G. Milliken, E. Plautz, R. Nudo, "Distal forelimb representations in primary motor cortex are redistributed after forelimb restriction: a longitudinal study in adult squirrel monkeys.", *J Neurophysiol*, 2013

[5] R. Nudo, B. Wise, F. SiFuentes, G. Milliken, "Neural substrates for the effects of rehabilitative training on motor recovery after ischemic infarct", *Science*, 1996

[6] L. Morgenstern, L. Lisabeth, A. Mecozzi, M. Smith, P. Longwell, D. McFarling, J. Risser, "A population-based study of acute stroke and TIA diagnosis", *Neurology*, 2003

[7] M. Bear, B. Connors, M. Paradiso, "Neuroscience", *Lippincot Williams & Wilkins*, 2007

[8] E. Niedermeyer, F. da Silva, "Electroencephalography: Basic Principles, Clinical Applications and Related Fields", *Lippincot Williams & Wilkins*, 2004

[9] M. Santello, M. Bianchi, M. Gabiccini, E. Ricciardi, G. Salvietti, D. Prattichizzo, M. Ernst, A. Moscatelli, H. Jörntell, A. Kappers, K. Kyriakopoulos, A. Albu-Schäffer, C. Castellini, A. Bicchi, "Hand synergies: Integration of robotics and neuroscience for understanding the control of biological and artificial hands", *ScienceDirect*, 2012

[10] J. Doyle, M. Botte, "Surgical Anatomy of the Hand and Upper Extremity", *Lippincot Williams & Wilkins*, 2003

[11] L. Bonini, F. Serventi, S. Bruni, M. Maranesi, M. Bimbi, L. Simone, S. Rozzi, P. Ferrari, L. Fogassi, "Selectivity for grip type and action goal in macaque inferior parietal and ventral premotor grasping neurons", *Journal of Neurophysiology*, 2012

[12] G. Scheslinger, "Der Mechanische Aufbau der kunstlichen Glieder", *Springer*, 1919

[13] M. Santello, "Control of hand muscles through common neural input", *Elsevier Science*, 2014

[14] A. d'Avella, F. Lacquaniti, "Control of reaching movements by muscle synergy combinations", *Frontiers in Computational Neuroscience*, 2013

[15] M. Santello, G. Baud-Bovy, H. Jörntell, "Neural bases of hand synergies", *Frontiers in Computational Neuroscience*, 2013

[16] N. Bernstein, "The coordination and regulation of movements", *Pergamon Press*, 1967

[17] G. Gottlieb, "A computational model of the simplest motor program", *Journal of Motor Behaviour*, 1993

[18] J. Scholz, G. SchÃűner, "The uncontrolled manifold concept: identifying control variables for a functional task", *Springer-Verlag*, 1999

[19] K. Pearson, "On Lines and Planes of Closest Fit to Systems of Points in Space", *Philosophical Magazine*, 1901

[20] H. Hotelling, "Analysis of a complex of statistical variables into principal components", *Journal of Educational Psychology*, 1933

[21] I. Jolliffe, J. Cadima, "Principal component analysis: a review and recent developments", *Philosophical Transactions R. Soc. A*, 2016

[22] F. Castells, P. Laguna, L. Sörnmo, A. Bollmann, J. Roig, "Principal Component Analysis in ECG Signal Processing", *EURASIP Journal on Advances in Signal Processing*, 2007

[23] A. Smeragliuolo, J. Hill, L. Disla, D. Putrino, "Validation of the Leap Motion Controller using markered motion capture technology", *ScienceDirect*, 2016

[24] Leap Motion API Overview, `https://developer.leapmotion.com/documentation/java/devguide/Leap_Overview.html`, 2015

[25] Leap Motion - How does the controller work?, http://blog.leapmotion.com/hardware-to-software-how-does-the-leap-motion-controller-work/, 2015

[26] Leap Motion SDK, http://blog.leapmotion.com/getting-started-leap-motion-sdk/, August 2014

[27] E. Niedermeyer, F. Lopes da Silva, "Electroencephalography: Basic principles, clinical applications and related fields", *Williams & Wilkins*, 1993

[28] M. Teplan, "Fundamentals of EEG measurement", *Measurement Science Review*, 2002

[29] F. Tyner, J. Knott, "Fundamentals of EEG technology", *Raven press*, 1989

[30] G. Pfurtschellera, F. Lopes da Silva, "Event-related EEG/MEG synchronization and desynchronization: basic principles", *Elsevier Science*, 1999

[31] C. Toro, G. Deuschl, R. Thatcher, S. Sato, C. Kufta, M. Hallett, "Event-related desynchronization and movement-related cortical potentials on the ECoG and EEG", *Elsevier Science*, 1994

[32] H. Agashe, A. Paek, Y. Zhang, J. Contreras-Vidal, "Global cortical activity predicts shape of hand during grasping", *Frontiers in Neuroscience*, 2015